

# Additively Manufactured Nanotechnology and Origami-enabled Flexible Microwave Electronics

Jimmy Hester, *Student Member, IEEE*, Sangkil Kim, *Student Member, IEEE*, Jo Bito, *Student Member, IEEE*, Taoran Le, *Student Member, IEEE*, John Kimionis, *Student Member, IEEE*, Daniel Revier, *Student Member, IEEE*, Christy Saintsing, *Student Member, IEEE*, Wenjing Su, *Student Member, IEEE*, Bijan Tehrani, *Student Member, IEEE*, Anya Traille, *Student Member, IEEE*, Benjamin S. Cook and Manos M. Tentzeris, *Fellow, IEEE*

**Abstract**—Inkjet printing on flexible paper and additive manufacturing technologies (AMT) are introduced for the sustainable ultra-low-cost fabrication of flexible radio frequency (RF)/microwave electronics and sensors. The paper covers examples of state-of-the-art integrated wireless sensor modules on paper or flexible polymers and shows numerous inkjet-printed passives, sensors, origami and microfluidics topologies. It also demonstrates additively manufactured antennas that could potentially set the foundation for the truly convergent wireless sensor ad-hoc networks of the future with enhanced cognitive intelligence and “zero-power” operability through ambient energy harvesting and wireless power transfer. The paper also discusses the major challenges for the realization of inkjet-printed/3D printed high-complexity flexible modules as well as future directions in the area of environmentally-friendly “Green” RF electronics and “Smart-House” conformal sensors.

**Index Terms**—Inkjet-printing, additive manufacturing, origami, nanotechnology, flexible electronics, RF, wireless sensors, microfluidics, passives, antennas, modules

## I. INTRODUCTION

PRINTING technologies have been playing an ever increasing role as fabrication methods over the last decade, especially in the growing field of flexible electronics because of their low operation cost, their ability to deal with flexible substrates, their capacity to work in large-area roll-to-roll (R2R) approaches and their inherent environmental friendliness [1]. Indeed, printing processes such as gravure printing, screen printing and inkjet printing are strictly additive and therefore do not waste much (if any) material.

Research towards the development of flexible electronics is very active at all levels, from the physical characterization of printed materials, the development and improvement of printed optoelectronic components and transistors to the integration of such components into fully printed flexible systems such as flexible displays and wearable and portable devices [2].

Such flexible and conformal wireless systems could play a vital role in the implementation of networks of a new range of low cost, wireless, “smart”, autonomous and therefore self-sustainable from a power perspective or, as we call it, “zero power”, devices capable of sensing, communicating measurement data and featuring unique identification capabilities.

However, printing techniques are not unique as many of their advantages are shared with the family of additive manufacturing technologies (AMT). These technologies can be seen

as the extension of 2D printing technologies to the 3<sup>rd</sup> spatial dimension. Each material layer is deposited on top of the previous in order to form truly 3D structures. These processes are also strictly additive, can accommodate large surfaces or volumes, thus being also very cheap and eco-friendly. AMTs are capable of producing flexible, conformal and rollable devices by printing flexible materials, especially in the light of the new possibilities offered by the use of the 3<sup>rd</sup> dimension and their capacity of depositing new nanotechnology-enabled materials with mechanical and physical properties unavailable in the realm of 2D printing.

In this paper, we will first discuss in Sec. II the properties and advantages of AMTs for the fabrication of flexible wireless electronics. In Sec. III we will then present various flexible wireless component prototypes fabricated with AMT. Sec. IV reports preliminary printed sensor modules, such as inkjet-printed nano-carbon-enabled gas and microfluidic sensors. Fully assembled RF nodes and modules (radar, beacon) are presented in Sec. V, while major challenges and future directions for the implementation of AMT-fabricated “zero-power” green flexible RF systems are discussed in Sec. VI.

## II. ADDITIVE MANUFACTURING TECHNOLOGIES (AMT)

### A. Inkjet printing

As previously argued, printing technologies started getting used due to their inherent capability of low-cost fabrication of devices using a wide range of materials on flexible substrates, in an environmentally friendly manner while being compatible with the strict quality requirements of multilayer components up to millimeter-wave frequencies.

Inkjet printing, in particular, has the specificity of being a printing method but also part of the AMT. Indeed, once the design file has been created, the inkjet printer can directly start depositing the ink layer by layer to fabricate it with no intermediate steps required. Furthermore, a wide range of materials can be deposited with precise layer-to-layer alignment with resolutions sufficient for operation up to sub-THz frequency range. For these reasons, it has been considered as one of the most promising manufacturing technologies for flexible wireless/RF devices and systems.

This strictly additive process, in most cases, works in a “Drop on Demand” (DOD) manner similar to that used in office inkjet printers. In DOD inkjet fabrication, small drops of ink loaded with the material to be deposited are generated

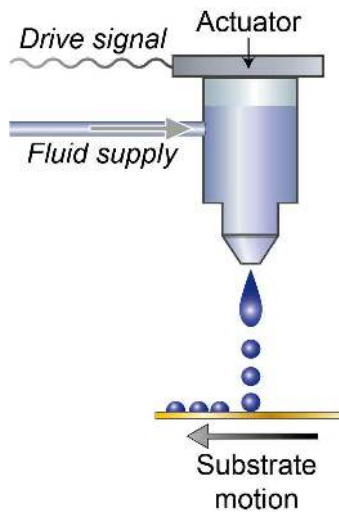


Fig. 1. DOD Material Jetting

by inkjet nozzles and projected toward the substrate (Fig. 1). The nozzles and/or substrate are moved to place the droplets of ink in specific places to generate the desired pattern. Upon hitting the substrate, the drop solvent, which is suspending the material to be deposited, evaporates from and/or absorbs into the substrate leaving the patterned material. Unlike standard photolithography methods that are subtractive and generate large amounts of chemical wastes, the only material wasted in this process is the solvent which can be recycled through ventilation systems. As a consequence, inkjet printing has an extremely low environmental footprint as a fabrication method. This simple process also gives a huge amount of versatility as to what materials can be printed and what substrate or object they can be printed onto.

The recent advancements in this manufacturing technology have been mostly driven by progress in the ink technology. Silver nanoparticle inks have now been used for more than a decade to print traces with conductivity values in the order of magnitude of screen printing techniques [3]. It is now possible to print dielectric polymers (such as PVP, PMMA, SU8, etc.) that have enabled the fabrication of fully inkjet-printed multilayer components [4]–[8] such as the ones that will be shown later on in this paper. All these layers of different materials can be deposited with high definition and precise alignment.

Furthermore, inkjet printing offers the unique capability of depositing in room temperatures precise quantities of nanoparticles (such as carbon nanoparticles) on flexible substrates to take advantage of their “sensing” semi-conducting properties. It has to be stressed that materials such as carbon nanotubes (CNT) require temperatures higher than 500 °C to be deposited with common fabrication processes, such as chemical vapor deposition (CVD) [9]. Most commonly used flexible dielectric substrates for radio frequency electronics can only tolerate temperatures up to, at most, 400 °C and therefore cannot be used with CVD of CNTs, a problem that does not exist with inkjet printing. This versatility is a reason why inkjet printing is very widely utilized by material scientists and serves

as a major cross-disciplinary interface where innovations in materials can readily enter the realm of electrical engineers for system integration.

Moreover, inkjet printing offers very good deposition definition. Features and gaps of 50 μm can be readily achieved even with entry level prototyping inkjet printers such as the Dimatix DMP-2800, while much lower values around 10 μm have been reported through surface treatment approaches. Last but not least, this fabrication process is extremely cheap due to the low cost of flexible substrates, the extremely small volume of the used ink and the lack of a clean room requirement.

### B. 3D material jetting

As demonstrated, inkjet printing is a leading technique in the fabrication of flexible conductive traces and thin/thick dielectrics due to its low material volume requirements and R2R processing capability, which naturally lends itself to straightforward integration with similar 3D structure jetting technologies for the local realization of below 100 μm detailed features.

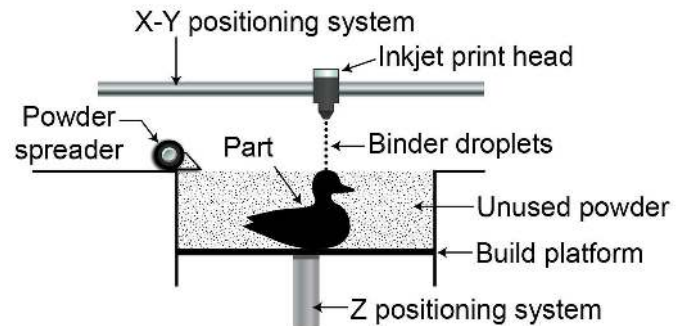


Fig. 2. Binder Jetting

Popularized by companies like Objet (now Stratasys) and ExOne, the jetting technology for 3D structures is well known for being robust, scalable and able to handle multi-material concepts well. In addition to the more traditional inkjet printing that has already been described, the material jetting side of AM can be broken into two more branches, material jetting and binder jetting. Material jetting typically relies on photopolymers to build up 3D structures. As the print head moves over the part-building area, small droplets are deposited and cured via UV light to solidify, in situ, before another pass is performed. Layer-by-layer, this section is gradually built up until completion. In contrast, binder jetting (Fig. 2) simply prints a glue above a powder bed. After every pass, a fresh layer of powder particles is spread evenly across the top and the next layer is “glued” to the previous layer, essentially “gluing” millions of particles of sand together to realize the desired shapes.

As has been already discussed, both 3D jetting techniques offer great benefits in terms of precision, cost, and environmental impact; only the material that is necessary is printed. A key advantage that these 3D jetting technologies offer is the added benefit of complex multi-material interactions. The Objet line of printers can, not only, print in multiple

colors, but can also provide multiple different strengths of material combinations in the complete range of 100% of one material and 0% of the other, to the complete opposite. This can be best visualized by looking at Fig. 3 of a multi-color figurine. Instead of using materials with different colors, this technique could be adapted for materials of Radio Frequency (RF)/Electromagnetic (EM) interest including magnetic, dielectric, sensing, piezoelectric materials. Several of these printers already have the capability of printing both very rigid and very flexible materials. Years of research and experience have been devoted to mixing and printing flexible parts meaning that custom flexible substrates could be printed on-the-fly for different components. Furthermore, binder jetting features the added benefit of removing the material (the powder) from the jetting process completely. This means that many materials that cannot be jetted can still be utilized if put into a powder form [10].



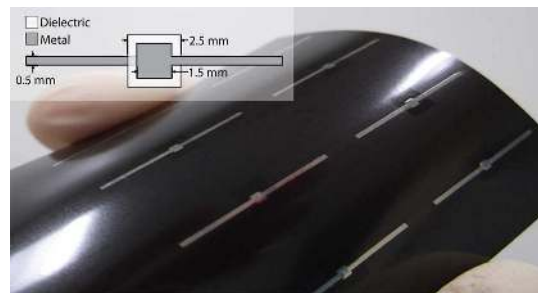
Fig. 3. Example of a multicolor/multimaterial single-print object taken from Stratasy

### III. ADDITIVELY MANUFACTURED RF COMPONENTS

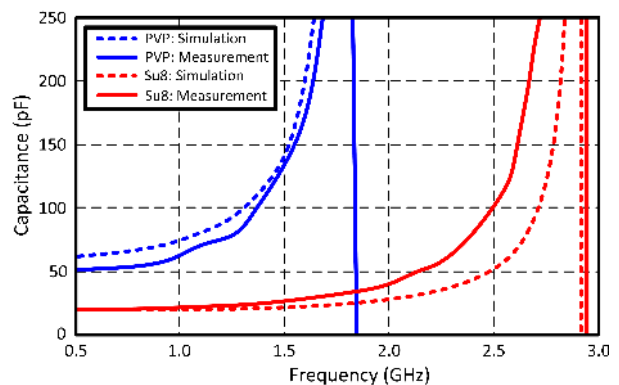
#### A. Inkjet-Printed Inductors and Capacitors

In order to realize any practical RF system, certain passive components are required. Capacitors and inductors play a crucial role in wireless and microwave systems by providing such elements as antenna-to-system impedance matching circuits, signal band-pass and band-stop filters, and discrete reactive components. The integrity of these components are typically outlined in three parameters: capacitance/inductance, self-resonant frequency (SRF), and quality factor. The integration of these passive components with inkjet printing allows for simple integration with flexible and conformal wireless systems, therefore eliminating the need of bulky external components, that would be easily delaminated for practical radii of curvature.

1) *Metal-Insulator-Metal Capacitors:* The most common variety of capacitor design typically used for low-profile reconfigurable applications and easily configurable applications is the metal-insulator-metal (MIM) capacitor. The simplicity of the design, where a single dielectric film separates two metallic plates, leads to a lot of flexibility in the plate area design, dielectric material characteristics, and even the possibility of multilayer stack-ups. This design scheme can be easily implemented with the inkjet printing fabrication process with the whole geometry (metal plates, thin dielectrics)



(a)



(b)

Fig. 4. (a) Fully inkjet-printed capacitors on a flexible Kapton substrate. (b) Capacitance simulation and measurement curves for thin (PVP) and thick (SU-8) printed dielectrics.

being fully printed. Several demonstrations have shown fully printed capacitors with either flexible substrate integration or SRFs reaching into the GHz range, yet what is desired is a combination of these two important facets [11]–[13].

Recent work with inkjet printing has achieved highly efficient MIM capacitors on flexible organic substrates, offering high SRFs suitable for RF applications and a capacitance per unit area comparable with that of bulk capacitors [6]. Using PVP-based (thinner layer hence higher capacitance) and SU-8-based (thicker layer hence lower capacitance) polymeric inks to realize thin and thick dielectric films with thicknesses of 0.8  $\mu\text{m}$  and 4  $\mu\text{m}$ , respectively, along with a highly conductive silver nanoparticle-based metallic ink, these capacitors are fabricated on a flexible Kapton substrate, shown in Fig. 4(a). The capacitance measurements of the capacitors versus frequency, shown in Fig. 4(b), demonstrate a similar effect of using thin and thick dielectrics on the overall capacitance of the component. SRF is also reported for each capacitor to exceed 1 GHz, entering the regime of high-frequency wireless and microwave electronics.

2) *Spiral Inductors:* The second flexible passive component to be realized through inkjet printing is the inductor. The most common implementation of RF inductors, typical in CMOS technology and other low-profile applications, is the spiral inductor. Typical designs of such inductors are realized through a physical spiraling of a metallic conductor and the utilization of a dielectric bridge to direct the conductor out from the center of the spiral. Several demonstrations of meander-line and spiral inductors have been proposed with inkjet printing

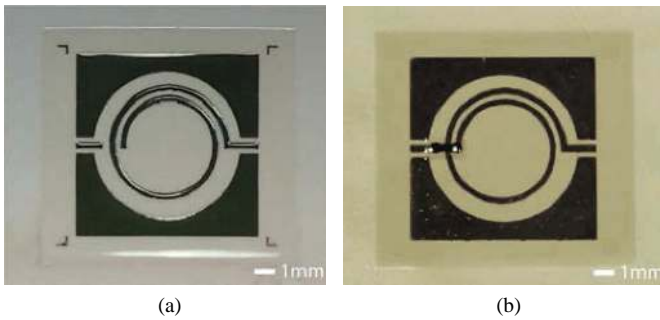


Fig. 5. Fabricated samples of inkjet-printed flexible spiral inductors (a) before and (b) after dielectric bridge deposition.

fabrication, yet many suffer from a low quality factor (Q) [14] and a low frequency operational restrictions [15], [16]. These implementations suffer mostly from fabrication limitations in the printed dielectric bridge thickness, where a thinner bridge has the potential to introduce a detrimental parasitic capacitance to the inductor element.

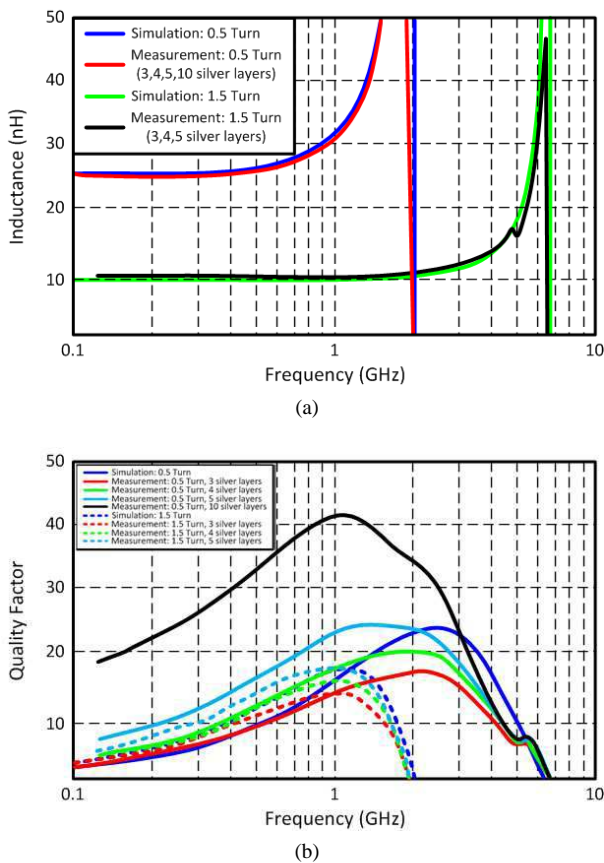


Fig. 6. (a) Inductance and (b) Quality factor measured and simulated values for different number of turns and metal thicknesses (500 nm per layer)

Through the introduction of a printable thick SU-8 dielectric ink, spiral inductors can be realized through a fully additive inkjet-printed method on flexible substrate [7]. The printing process includes the deposition of a conductive spiral, followed by a 24 $\mu$ m thick dielectric bridge with via holes that is complemented with an overlying conductive trace effectively connecting the printed spiral to the output trace. Fabricated

1.5 turn inductor prototypes before and after bridge fabrication are shown in Fig. 5. This fully printed thick dielectric bridge allows for a smaller parasitic capacitance, thus leading to the realization of higher inductance values for a given SRF. Fig. 6(a) shows the equivalent inductance of 0.5 and 1.5 turns designs. The quality factor of the printed inductors, shown in Fig. 6(b), varies from 8.5 to 21 at 1 GHz, depending on the number of silver nanoparticle layers printed, demonstrating the highest quality factor and inductance values reported in printed passives literature. Multiple iterations of inductor fabrication demonstrates a repeatability within 5% for both inductance and SRF, showing great promise for fully printed RF modules. The combination of these fully printed high-Q inductors and highly scalable capacitors help define a basis for performance low-cost and flexible RF electronic systems through inkjet printing.

*B. Flexible Interconnects, Metamaterials and Isolating Structures*

It is very common for flexible RF electronics and modules to be mounted or wrapped around curved lossy (e.g. human body mounted wearable electronics) or metallic structures (e.g. bridge-mounted structural health monitoring sensors). Thus, there is a necessity for highly efficient and durable flexible interconnects isolating structures, such as artificial magnetic conductors and frequency-selective-surfaces utilizing metamaterial architectures in order to maximize the communication range and optimize the RF performance in typical rugged scenarios. This section discusses various additively manufactured structures of these types stressing major large-area implementation challenges.

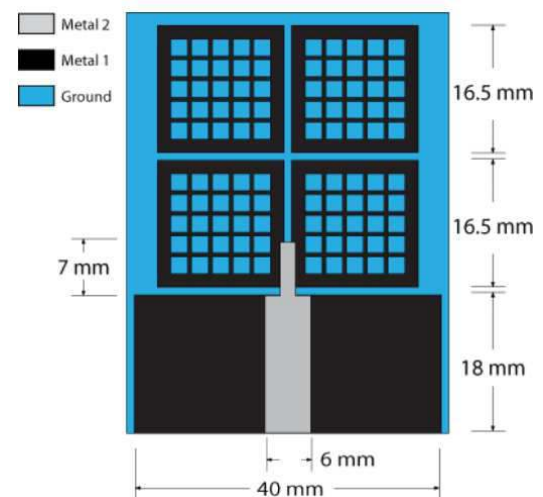


Fig. 7. AMC backed monopole antenna [17]

*1) A Printed Flexible Artificial Magnetic Conductor (AMC) for Wearable Application:* In numerous practical applications with highly lossy or conductive mounting structures, the spacing between the thin-substrate RF components and the mounting structure themselves plays a critical role on the excited modes of wave propagation as well as on the effective range of the wireless system. This is especially true for radiating elements such as antennas, especially when mounted

high-permittivity lossy materials, such as the human body ( $\epsilon_r > 30$  [18]). This detrimental effect is commonly referred as ‘detuning’ of the component. It is possible to tackle this issue by designed patterned isolation structures, such as Artificial Magnetic Conductors (AMC), that can be placed between the component and the mounting structures.

To demonstrate the capability of inkjet printing process to realize low-cost flexible large-area isolating structures, an inkjet-printed AMC-backed flexible monopole antenna for wearable applications was introduced in [17]. A waffle-like unit cell AMC was inkjet-printed on low-cost flexible paper, and a microstrip line-fed monopole antenna was mounted on top of this periodic structure, as shown on Fig. 7.

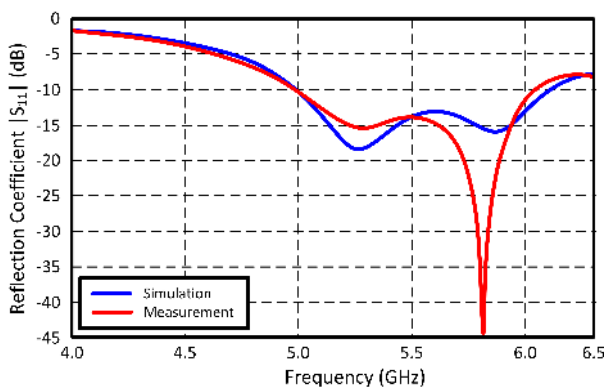


Fig. 8. Reflection coefficient  $S_{11}$  (measured and simulated) of the AMC backed monopole [17]

The simulated and measured reflection coefficients (Fig. 8) and radiation patterns (Fig. 9) of the antenna show good agreement over the WiFi band around 5-6 GHz. The gain values of the antenna measured ‘on’ (folded around a human phantom) and ‘off’ (free space) of a human phantom (Fig. 10) show virtually no difference and therefore demonstrate how the flexible AMC, on top of improving the performance of this non-grounded antenna, isolates it from highly lossy materials that it may be placed on. This opens the possibility to print a broad range of flexible high-performance antenna designs for wearable applications.

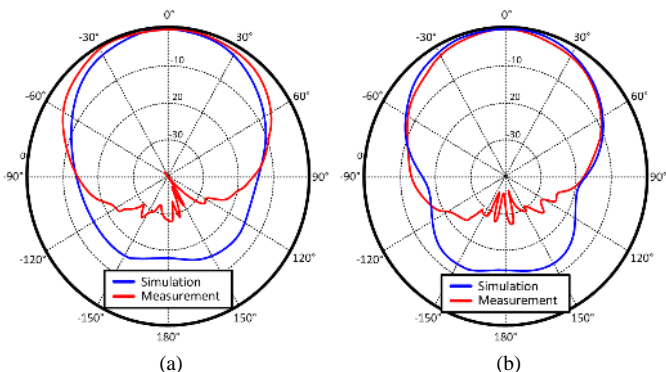


Fig. 9. Radiation patterns (measured and simulated) of the AMC backed monopole at (a) 5 GHz and (b) 6 GHz [17]

2) *Flexible Printed Metamaterial Absorber*: A novel inkjet-printed metamaterial absorber is introduced for the first time in [19]. Unwanted electromagnetic (EM) waves in specific frequency bands can be typically dissipated and absorbed by EM absorbers to suppress undesirable reflections from dielectric/metallic boundaries [20]. Conventional material-based absorbers are bulky, heavy and high-cost. However, the inkjet-printed metamaterial-based absorbers on paper are low-cost, flexible, and low-profile due to the additive and cost effective properties of inkjet printing [21], [22]. The designed EM absorber prototype is making use of a frequency selective surface (FSS) structure which consists of a periodic resonator structure backed by a conductor. Therefore, it is possible to achieve a more low-profile flexible metamaterial structure than conventional absorbers while maintaining high absorptivity.

The geometry of a unit cell of the presented absorber’s periodic structure, which consists of circular Jerusalem-Cross resonators, is demonstrated in Fig. 11(a). The designed absorber consists of circular Jerusalem-Cross resonators and is inkjet-printed on paper. The absorber prototype was inkjet-printed on paper and was composed of 15x15 unit cells on a 0.5 mm thick paper as shown in Fig. 11(b). The flexibility of the printed absorber is shown in Fig. 11(c). The amount of absorbed power (dissipated power by the EM absorber) is shown in Fig. 12. with a peak value of measured absorptivity equal to 79.5% at 10.36 GHz. The discrepancy between the simulation and the measurement results are attributed to the surface roughness of the fabricated EM absorber. Indeed, the reported surface roughness of photo paper is about 1  $\mu\text{m}$  and the polymeric surface of paper experiences mechanical stress during the thermal sintering and bonding process [5].

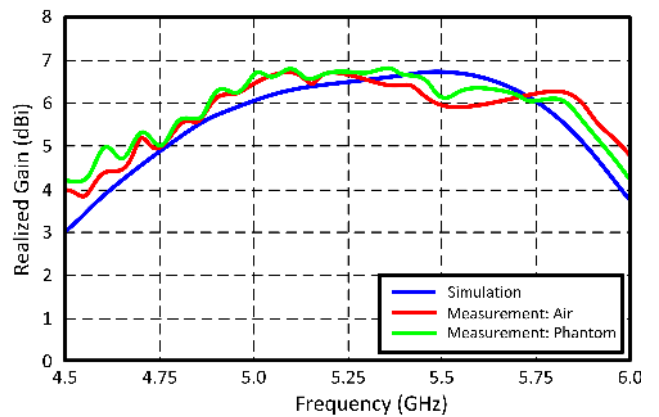


Fig. 10. Gain of the printed flexible AMC-backed monopole (simulated, measured in free space and measured on a human phantom) [17]

3) *An Inkjet-Printed Flexible Via-Hole Interconnect and a flexible Substrate Integrated Waveguide (SIW)*: Interconnects play a critical part in the performance of integrated RF modules as well as in the realization of low-EMI/EMC substrate-integrated waveguide structures. Flexibility requirements further complicate the design of RF interconnects, as they typically create cracks and local discontinuities enhancing local reflections and exciting local standing waves. In this subsection, a novel flexible via fabrication process utilizing inkjet printing technology is presented. In previously reported

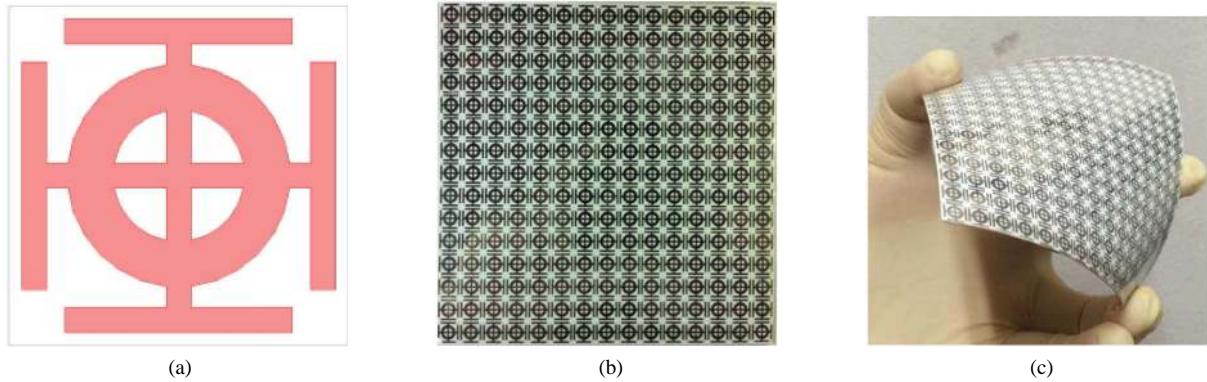


Fig. 11. (a) Geometry of a unit cell, (b) fabricated absorber, and (c) flexibility of the absorber.

efforts, inkjet-printed via holes have been successfully implemented on very thin substrates [23]–[25]. The stepped via approach shown here (with a 2 mm diameter) achieved the thickest via (1 mm long) while demonstrating a good via resistance of  $7.4 \pm 2 \Omega$  compared to prior approaches despite the fact that it is very challenging to metalize via holes on relatively thick substrates. If the via holes were metalized with a similar approach to other inkjet-printed structures, i.e. printing multiple layers on drilled via holes, it would result in detrimental discontinuities. The printed silver nanoparticles fail to form a continuous metal layer on the straight via hole configurations due to the shrinkage of the silver ink during the sintering process because of the resulting evaporation of the solvents, the polymers (a dispersant on the silver nanoparticles) and the impurities of the ink. Gravity further enhances the downward shrinkage of the ink, which results in cracks on the metalized via wall. A stepped via hole is introduced in order to create a gradual transition between the top and the bottom planar substrate surface and reduce the stress on printed silver nano-particles on the via hole during the sintering process, that are typically detrimental for the performance of uniform vias as reported previously. The fabrication process is shown in detail in Fig. 13.

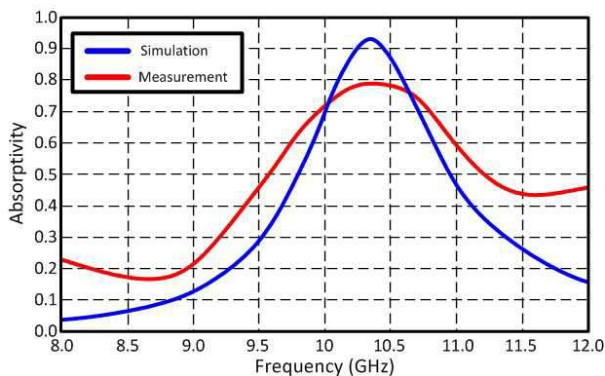


Fig. 12. Simulated and measured absorptivity of the inkjet-printed absorber prototype.

This novel flexible via-hole fabrication process was also utilized to realize a fully inkjet-printed flexible Substrate Integrated Waveguide (SIW) on polyimide (thickness: 250  $\mu\text{m}$ )

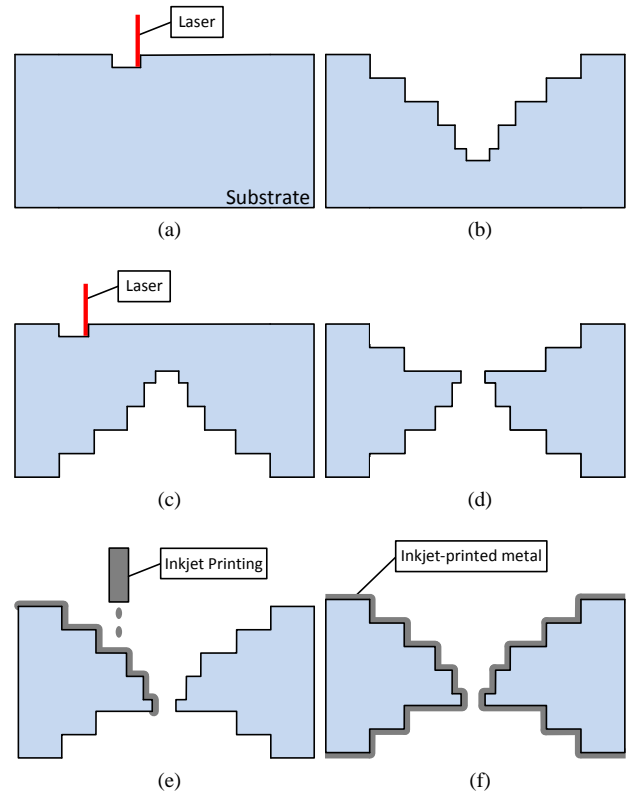


Fig. 13. Fabrication process of the flexible via interconnect with laser etching of one side ((a)→(b)) followed by laser etching of the other side ((c)→(d)) and inkjet printing of nanoparticle conductive ink on the top (e) and then on the bottom half area (f).

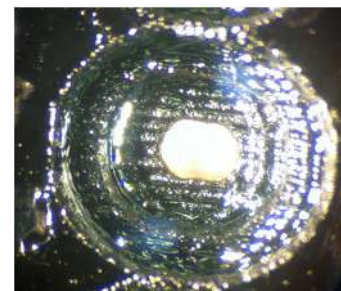


Fig. 14. Fabricated stepped via hole (magnification ratio: x10)

as demonstrated in [26]. The geometry of a microstrip-SIW-microstrip (back-to-back microstrip-SIW transitions) benchmarking transition is shown in Fig. 15(a) with the dimensions of the transition and the vias being optimized to minimize the radiation leakage, the insertion loss, and the fabrication error.

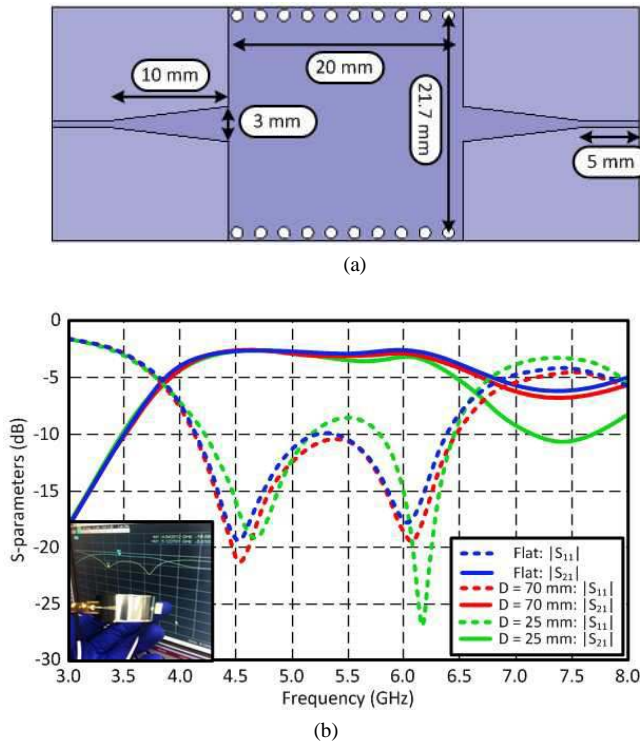


Fig. 15. (a) Geometry of the benchmarking microstrip-SIW-microstrip transition. (b) Flexibility test of the fabricated flexible transition prototype (D is radius of curvature) [26].

The flexibility of the SIW interconnect is experimentally demonstrated as shown in Fig. 15(b). The fabricated SIW interconnect was wrapped around cylinders with diameters ranging from 25 mm to 70 mm. The measured frequency responses for all different radii of curvature ( $S_{11}$  &  $S_{21}$ ) have shown good repeatability and robustness since the measured S-parameters have been almost identical before and after the bending test. This demonstrates that it is even possible, using the via fabrication method previously presented, to fully inkjet print flexible via-enabled RF structures (e.g. broadband transitions, waveguides) that remain functional under various bending, flexing and rolling conditions.

### C. Flexible “Origami” Reconfigurable Antennas

Traditional antennas lack the ability to adapt to changing system requirements by virtue of their design, since their operating characteristics are fixed. Introducing reconfigurability to an antenna can improve system performance and/or reduce the required number of antennas for a particular application. Reconfigurability is the capacity to change a radiator’s operating characteristics, such as frequency of operation, impedance bandwidth, and radiation pattern. Reconfigurable antennas have been in existence since the early 1930’s, when the nulls of a two-element array were steered by a phase changer to

determine the arrival direction of a signal [27]. The most common methods utilized to achieve reconfigurability have since been through the use of phase shifters, attenuators, diodes, tunable materials, active materials, microelectromechanical structures (MEMS) or mechanical methods via moving parts [28]. However, a novel way of achieving reconfigurability taking advantage of “origami-based” shape changing enabled by a combination of inkjet printing and AMT on flexible materials is presented in this subsection.

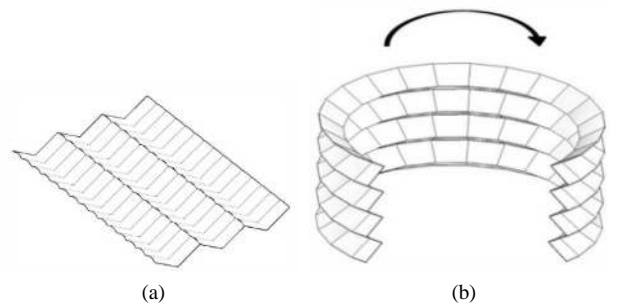


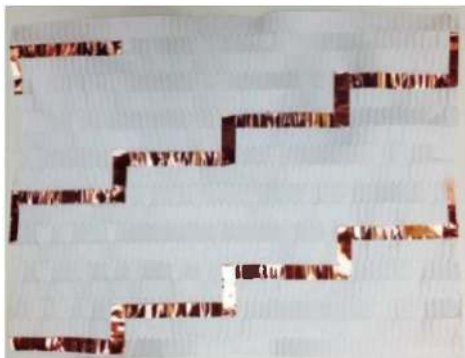
Fig. 16. (a) “Origami”-creased flexible base material (b) Folding of a flexible deployable accordion lantern structure [29].

The introduction of deployable origami structures has introduced new methods for shelter construction [30], biomedical applications [31], and space applications [32]. These structures enable expanded and compressed “end” states and numerous in-between states. Deployable structures, such as the one shown on Fig. 16 and Fig. 17, hold much promise for use in flexible reconfigurable antennas.

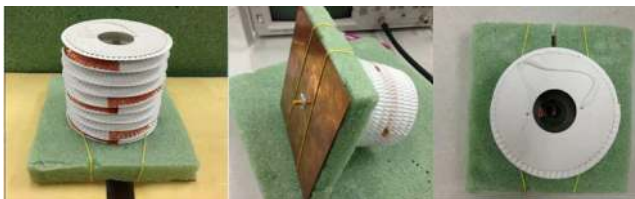
As a first proof-of-concept demonstration, a flexible reconfigurable “origami-based” axial-mode helical antenna which can change its operating frequency bands through its height modification has been created [33] with a structure shown in Fig. 18, while Fig. 19(a) and Fig. 19(b) show the simulated and measured return loss at the compressed and expanded states.

Kirigami is a derivative of origami which involves cutting and gluing in addition to traditional folding. A variety of other interesting shapes taking advantage of this method can be formed. For example, an inkjet-printed flexible reconfigurable spiral antenna incorporating this technique was created [34] on photo paper. The two end states are the equivalent of a planar spiral antenna and a conical antenna as shown in Fig. 20. As the flexible structure is telescoped into its conical shape, the gain of the antenna is effectively increased in real time.

Efforts are underway to take origami/kirigami inspired antennas one step further. Two drawbacks of current designs are the requirement for manual reconfiguration and the need of mechanical support structures for the stabilization of the different states. Traditional mechanical components could support this operation but tend to be bulky and require additional power. One cutting-edge solution implemented to alleviate this problem is the use of smart flexible materials [35]. For instance, a shape memory alloy (SMA) was utilized with a reconfigurable helical antenna to accomplish changes in height [36]. Applying a direct current (DC) through the SMA heats the material causing the SMA to contract, thereby reducing the height of the antenna. Once the current is removed, the



(a)



(b)

Fig. 17. (a) Flat paper with copper strip before folding (b) Assembled flexible reconfigurable accordion antenna. [29].

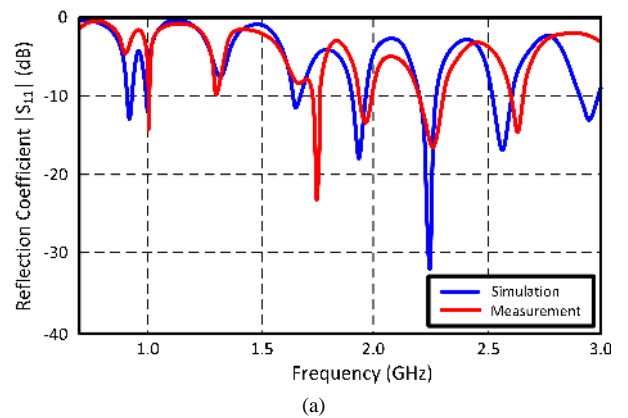


Fig. 18. Flexible helical antenna constructed on a deployable origami structure. [33]

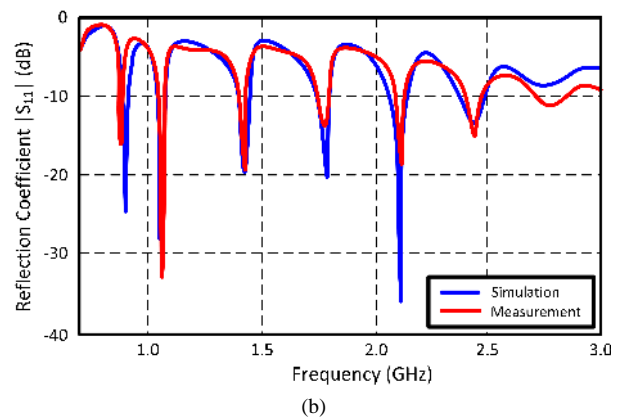
spring-like forces of the helix extends the structure back to its original height.

A revolutionary way of depositing flexible smart materials through additive manufacturing is a process termed “4D Printing” that uses a multi-material polymer printer to create printed active composites (PACs), which are 3D printed, with an added fourth dimension being a shape change effect [37]. Origami inspired boxes, pyramids, and airplanes have already been demonstrated by utilizing PAC hinges to achieve the folding.

Current research efforts are devoted to utilizing 4D printing to achieve partially self-actuated origami/kirigami-inspired flexible reconfigurable antennas, resonators and other RF structures. An Objet Connex 260 (Statasys, Edina, MN, USA) 3D multi-material polymer printer has been used for the fabrication of a proof-of-concept preliminary flexible prototype. Droplets of a polymer ink are initially deposited at a temperature of around 70 °C and then UV photo-polymerized.



(a)



(b)

Fig. 19. Reflection coefficient of the (a) compressed state, (b) expanded state of the flexible helical antenna of Fig. 18 [33]

Commercial inks TangoBlackPlus and VeroWhite are, currently, the most utilized materials for that purpose. The thermo-mechanical properties of the printed materials matrix can locally be selected by adjusting the ratio of the two materials. Hinges for origami-type flexible folds are created using a matrix with a higher content of TangoBlackPlus, which employs a lower glass transition temperature than VeroWhite. The printed configuration of the structure, also called the “permanent” state, can be changed to a “temporary shape” by heating the hinges past the associated glass transition temperature and applying a small mechanical force. Once the object is cooled to room temperature, it maintains its “temporary shape”. Reheating the body past the glass transition temperature of the hinges triggers a return to the permanent state.



(a)

(b)

Fig. 20. A kirigami-inspired reconfigurable spiral antenna. (a) Planar configuration and (b) conical configuration [34]



Fig. 21. A flexible 3D printed SMA cube with an inkjet-printed antenna on one of its faces

Fig. 21 shows the prototype of a cubic structure in its “temporary shape” with an inkjet-printed patch antenna on one of its faces.

Current efforts are focusing on coupling this polymer depositing AMT with conductor-depositing AMTs, such as inkjet printing, in order to create fully additively manufactured flexible reconfigurable antennas, such as the one shown on Fig. 21. Various printed Wireless Power Transfer (WPT) powered local heating topologies are also currently investigated for the wireless triggering of the shape changing effect of the flexible “origami”-based devices.

3D/4D printed flexible reconfigurable antennas can be easily launched in compact volumes and deployed on aircraft and space platforms (commercial or military) as a low-cost rollable/flexible alternative to current methods which are commonly bulky and non shape-reconfigurable. Wearable and implantable electronics and sensors can also benefit from such structures, as they cause only minimal - if any - interference with motion. Other potential applications could also include, among others, health and contamination monitoring, artificial limb control, and exoskeletons. Wireless systems with requirements for arbitrary orientation cognitive radio systems, and real-time reconfigurable wireless systems (e.g. structural health monitoring “smart skins”) could also benefit from this technology.

#### IV. FLEXIBLE INKJET-PRINTED SENSING STRUCTURES

One of the fastest growing areas of flexible RF/wireless modules is the area of wireless sensors. In addition to flexible passives, interconnects, isolation structures and antennas, previously presented, that enable the efficient wireless communication capabilities of such modules, it is very important to “seamlessly” integrate flexible sensing structures, such as microfluidics and nanotechnology-enabled sensing configurations. This section presents preliminary proof-of-concept flexible prototypes of microfluidic sensors that can be utilized to distinguish between different fluids based on their relative permittivity values and nanomaterial-based gas sensors that can be integrated into wireless nodes to enable them with chemical gas sensing and discrimination capabilities.

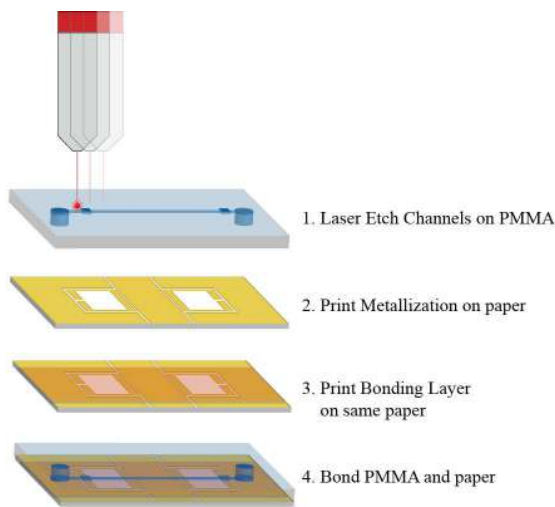


Fig. 22. Fabrication process of an inkjet-printed flexible microfluidic tunable filter / liquid sensor

#### A. Inkjet-Printed Flexible Microfluidic Tunable RF Structures & Sensors

Due to its inherent capability of manipulating extremely small quantities of liquid, microfluidics is an emerging technology that has been widely used in manufacturing control, biomedical sensing, chemical assay and lab-on-chip applications over the past decade. Lately, there have been numerous efforts to integrate flexible microfluidics with different RF designs to enable them with real-time liquid-controlled tunability. Specifically, in order to realize low-cost and environmental-friendly microfluidic devices on flexible paper and polymer substrates, the inkjet-printing manufacturing technique has been introduced as a reliable fabrication process, as shown in Fig. 22. In preliminary reported prototypes, the channel and the feed holes are laser etched into sheets of poly(methylmethacrylate)(PMMA). Fully inkjet-printed flexible microfluidic channels are under development and are expected to be reported in the near future. In the flexible prototype reported in [38], a Dimatix DMP-2800 series printer is used to inkjet print a silver nanoparticle ink onto the paper substrate. After curing the silver ink, a layer of polymer (SU-8) is printed over the metalized pattern to be used as an adhesive to seal the channel as well as the isolation layer between the filling fluids and the metalized pattern. Then the device is finalized by curing the SU-8 layer while applying pressure.

Such flexible microfluidic structures could be a useful tool to develop numerous flexible and tunable antennas, passives, resonators and filters. A metamaterial-inspired temperature stable inkjet-printed microfluidic-tunable bandstop filter, built by coupling a Split Ring Resonator (SRR) to a coplanar waveguide, is shown in the inserted figure in Fig. 23(b). By loading the capacitive gap of the SRR with a variety of fluids having different permittivities, the resonant frequency of the filter can be tuned with a high sensitivity of  $0.4 \text{ \%}/\epsilon_r$ , as shown in Fig. 23(a), which verifies this filter’s ability to distinguish different fluid or mixtures based on their permittivity. Moreover, the flexible fabricated filter demonstrates a high level of

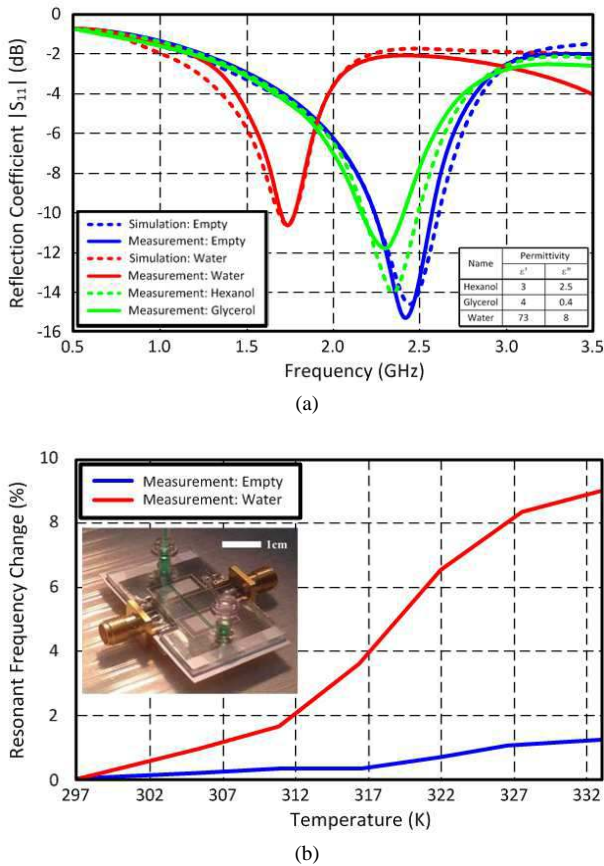


Fig. 23. (a) Measured and simulated insertion loss for different fluids pumped into the channel [39]–[41], (b) Resonant frequency shift due to the temperature change of the into the microfluidic channel.

temperature sensitivity, as shown in Fig. 23(b). For a 35 K temperature increase, a 9% increase of the resonant frequency for a water-filled device is demonstrated, which verifies the functionality of the liquid-tunable filter as a temperature sensor as well. The initial results could be easily extended to creating flexible fluid-tunable SRR metasurfaces which could be used in a vast array of applications ranging from in-vivo sensing to wide-dynamic-range tunable RF filters.

**B. Inkjet-Printed Flexible Carbon-Nanomaterial-Enabled Sensors**

1) *Fundamental Sensing Mechanism:* Carbon nanomaterials (e.g. CNT’s, graphene) have already found a very extensive use as sensing devices since they experience notable changes in their electrical properties (e.g. DC resistivity, dielectric constant, effective complex impedance) in the presence of particular substances. The underlying mechanism is their ability to selectively absorb various compounds on their surface, resulting in electron donating and accepting interactions. The resulting material properties changes can be exploited to determine the presence and concentration of various chemicals by translating them into measurable electrical quantities, such as changes in voltage, current, resonant frequency, and backscattered power amplitude. Typical excellent electrical conductivity values as well as an inherent ability to be easily functionalized for a wide range of chemicals make these novel

materials ideal candidates for the development of a broad spectrum of portable and wearable sensors. Moreover, the ability to deposit these materials via inkjet printing on low cost, flexible, environmentally friendly substrates opens the possibility of a scalable production of such flexible carbon-nanomaterial-enabled sensors. Multiple and differently functionalized sensors of this type could be easily integrated on a variety of flexible substrates, such as paper or polymer, with other previously reported RF flexible components thus featuring a combined capability of wireless communication and selective ambient sensing of a wide range of gases.

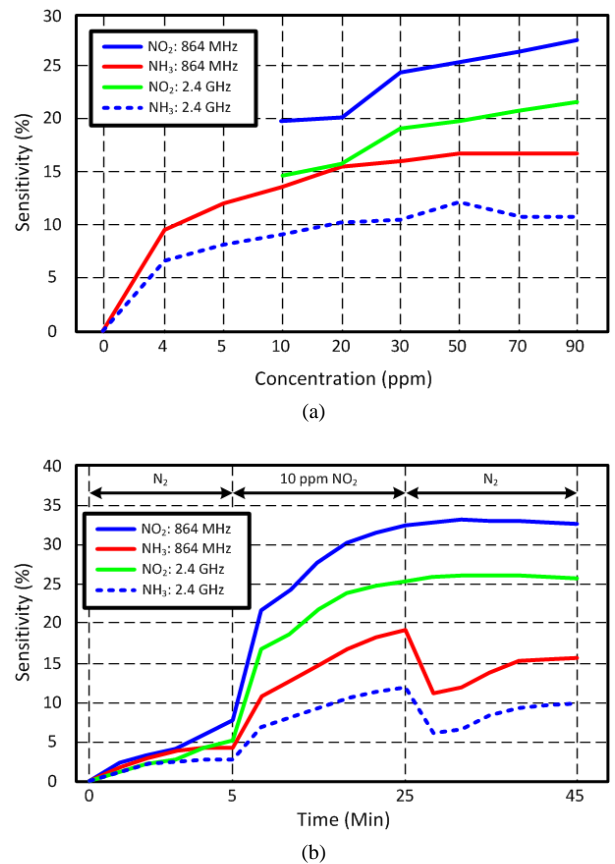


Fig. 24. (a) Flexible CNT sensor response as a function of the sensed gas concentration and (b) Time response in the presence of NH<sub>3</sub> and NO<sub>2</sub> using concentrations of 10 ppm at 864 MHz and 2.4 GHz.

2) *Flexible Carbon nanotube (CNT) based sensor prototype:* The first proof-of-concept prototype [42] presented in this section features the use of Multi Walled CNT’s (MWCNT) as the basis for a thin-film gas-sensing material, which was deposited using a water based MWCNT ink that was inkjet-printed on a flexible polyimide Kapton substrate.

NO<sub>2</sub> and NH<sub>3</sub>, diluted in N<sub>2</sub>, were chosen as the test gases due to their extensive industrial use, toxicity, and relative ease of acquisition. The effect of these gases on the MWCNT material properties was tested using a KIN-TEK FlexStream gas standard generator, which is capable of providing very stable and accurate analyte concentrations into a carrier gas down to very low concentrations, using gas permeation tubes of various gas delivery rates. The changes in the resistance of the tested sensor were monitored as a sensing indicator.

Before any test, an almost complete desorption of chemical species potentially previously absorbed by the sensing material was achieved by placing the sensors under a flow of pure nitrogen (N<sub>2</sub>) for 5 minutes.

Fig. 24(a) shows the sensitivity variation of the flexible CNT sensor as a function of the concentration of both test gases in the environment surrounding the sensor and at the two unlicensed frequencies of 864MHz and 2.4 GHz. The sensitivity is hereby defined as the change of the resistivity of the inkjet-printed CNT-based sensing patch as a function of time relative to its value at time t=0.

$$Sensitivity = \frac{R - R_0}{R_0} \quad (1)$$

where  $R_0$  is the resistance at time t=0. Sensitivities of 21.7% and 9.4% were achieved for 10 ppm NO<sub>2</sub> and 4 ppm NH<sub>3</sub>, respectively, at 864 MHz ; these values are higher than those achieved in recent efforts [43] for a higher concentration (100 ppm) of NH<sub>3</sub>. Fig. 24(b) shows the response over time to the same chemical gases at the chosen frequencies. For this portion of the experiment, 10 ppm was used as the concentration for both gas tests. As shown in Fig. 24(b), the MWCNT-based flexible gas sensor features a very fast response to both gases (less than 1 minute). After testing, the sensor exposed to NH<sub>3</sub> features a rapid recovery as well.

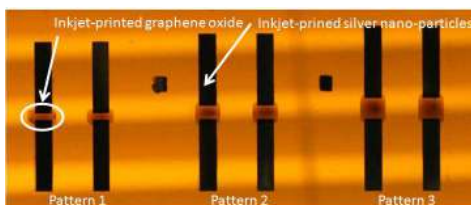


Fig. 25. Three different lengths of rGO patterns interfaced with inkjet-printed silver nanoparticle electrodes on flexible Kapton (referred to as patterns 1, 2 and 3, counted from left to right)

3) *A flexible inkjet-printed reduced graphene oxide (rGO) Based Sensor Prototype:* Recently reported rGO-based inks have enabled the implementation of flexible inkjet-printed graphene-based gas detection sensors featuring good recovery and response times as well as high sensitivity. In the prototype reported in [44], graphene oxide (GO), which is the precursor to graphene, is inkjet printed onto a UV-ozone treated Kapton substrate (Fig. 25). The printed GO is then post processed to reduce it to rGO. Sintering GO using heat and laser can be both used for this process. After applying 500 ppm of NH<sub>3</sub>, resistivity value changes of up to 6% were observed with response times of less than five minutes. Upon the removal of the gas at t=15 minutes and application of air, the sensors recovered by 30% within five minutes verifying the reusability of such flexible inkjet-printed sensors. Fig. 26(b) displays sensitivity values of the flexible sensing film for CO and NH<sub>3</sub> showing a noticeable difference in the characteristic response of the sensor to each gas, verifying the selectivity characteristics of these sensors.

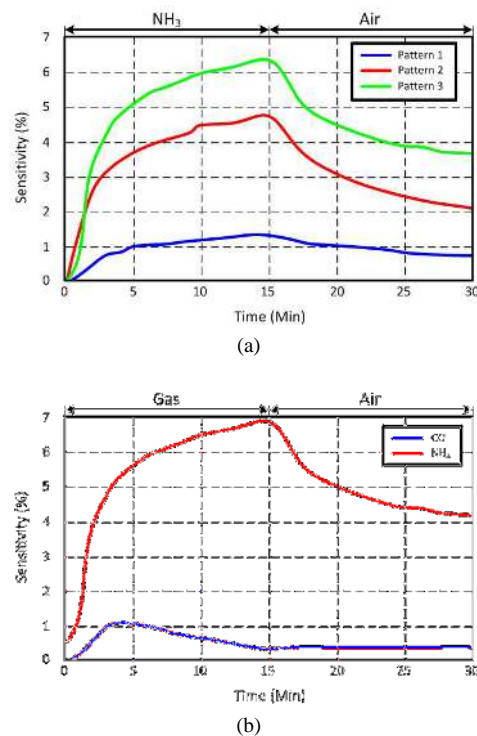


Fig. 26. (a) Measured response of the three flexible inkjet-printed rGO thin films shown on Fig. 25 in presence of NH<sub>3</sub>; (b) Measured response of the flexible rGO thin film (pattern 1) to NH<sub>3</sub> and CO.

## V. INTEGRATED RF SYSTEMS

### A. Flexible RF modules

The previous sections have focused on state-of-the-art flexible RF electronic and sensing components that have been fabricated using inkjet printing and other additive manufacturing techniques. Sec. V presents various flexible inkjet-printed RF integrated modules and systems ranging from a beacon oscillator and a rollable inkjet-printed Ground Penetrating Radar to a flexible printed reflection amplifier and various conformal wireless sensor nodes. Although some high-frequency active circuits [45] and logical circuits, such as low-frequency Radio Frequency IDentification (RFID) transponders [9], have been reported using a state-of-the-art inkjet printed thin-film transistor (TFT) technology, acceptable combinations of low power dissipation, high mobility (for use in higher frequencies than kHz), high on-off current ratio, small size and repeatable/scalable manufacturing have not yet been demonstrated for high-frequency flexible topologies. For these reasons, most reported flexible RF modules need to combine standard integrated circuits (IC) with the fully inkjet-printed flexible components previously presented.

1) *Flexible Inkjet-Printed Beacon Oscillator - Active antenna:* Numerous system-level hybrid printed electronics devices have been recently reported in [46], [47]. They are composed of additively manufactured passives, such as transmission lines, antennas, capacitors and inductors, with discrete active/nonlinear components (transistors, diode, etc) and high-performance CMOS chips on low-cost flexible substrates, effectively providing a flexible and cost-effective method for circuit fabrication, that simultaneously takes advantage of both

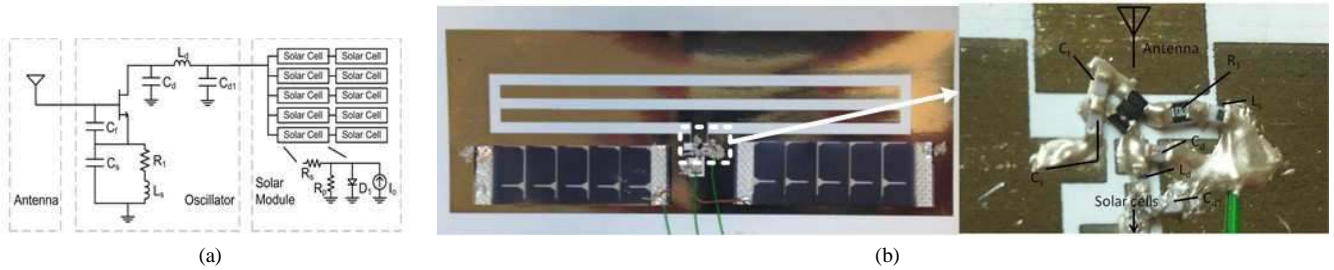
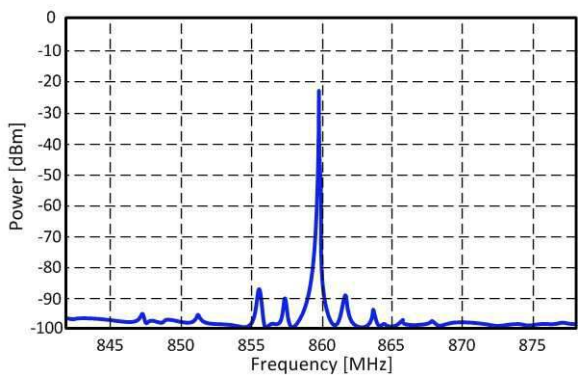
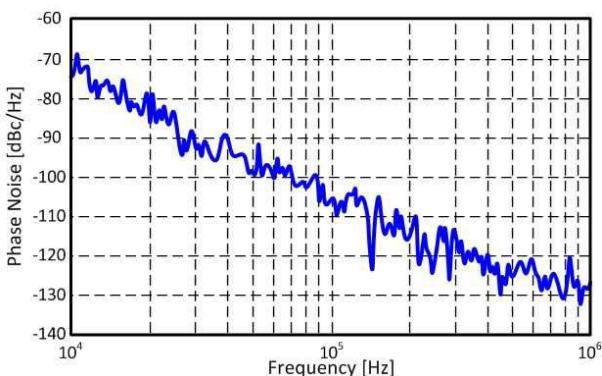


Fig. 27. (a) Circuit schematic and (b) fabricated flexible printed RF beacon oscillator prototype [46], [47].



(a)



(b)

Fig. 28. Measured (a) spectrum and (b) phase noise of the flexible RF beacon oscillator of Fig. 27 [47].

the unique features of both CMOS and AM/inkjet printing technologies. In [46], [47], a folded slot antenna along with a circuit layout were inkjet-printed on paper, and IC chips, such as JFET and a voltage regulator, were mounted on the printed circuit. These prototypes demonstrate the easy integration of active circuits with energy harvesters, such as a solar cell, utilizing inkjet printing technology and low-cost flexible substrates.

A proof-of-concept flexible RF beacon oscillator is shown on Fig. 27. It consists of 4 blocks: a solar module, a power regulator, an oscillator, and an antenna. The solar module, the power regulator, and the oscillator circuits were mounted on the inkjet printed circuit footprint by using a conductive epoxy. The autonomous module oscillates at 858 MHz (Fig. 28(a)) by continuously converting solar power to RF power, while a

phase noise value of  $-130$  dBc has been measured at 1 MHz away from the carrier frequency (Fig. 28(b)).

2) A Rollable/Flexible Printed Ground Penetrating Radar (GPR): Typical GPR systems transmit electromagnetic waves and then measure and analyze the multiple reflections in order to develop accurate subsurface mapping and detect buried objects. Environmental GPR systems use frequencies in the Very High Frequency (VHF) band to achieve large exploration depths through conductive soil layers ( $\epsilon_r \approx 3-15$ ,  $\sigma \approx 0.001-0.01$  S m $^{-1}$ ). The large antennas required, however, can complicate wide-area outdoor measurements which is why most systems are equipped with detachable antennas. A drastic improvement in portability can be achieved through the application of new flexible and rollable packaging approaches that would allow the entire system to be stored quickly and transported easily, while being easily re-deployed at the point of exploration. A flexible radar system that can be rolled into a compact container and attached to a backpack for easy transportation would reduce the cost of GPR implementations, particularly for measurements requiring a large staff to transport heavy equipment through remote places with extreme conditions as well as when requiring the use of multiple transmit/receive antennas for complex measurements. In the presented flexible radar prototype, inkjet printing technology is used to develop a monolithic radar system [48] in which the actives, passives and antenna should share a single roll-able substrate. This level of integration addresses various major challenges of realizing a flexible system when it comes to materials, processes and electrical design. For this particular application, the two-step electroless plating bath technology process was chosen. This process consists of the inkjet printing of a catalyst ink as a seed layer followed by copper deposition on top of the seed layer through the use of electroless copper bath deposition process. This approach was chosen due to its inherent wide-area printing capabilities and excellent adhesion properties [49], both of which are beneficial for the realization of a large flexible system which must roll around a tight radius.

The fabricated system prototype (Fig. 29(b)) features a basic Frequency-Modulated Continuous-Wave (FMCW) architecture that includes the Voltage Controlled Oscillator (VCO), coupler, Low Noise Amplifier (LNA), mixer and matching circuits chosen to implement the fundamental FMCW radar functions, that consist of a frequency sweep, amplification and conversion from RF to Intermediate Frequency (IF). The entire system was realized on a single layer of Polyethylene terephthalate

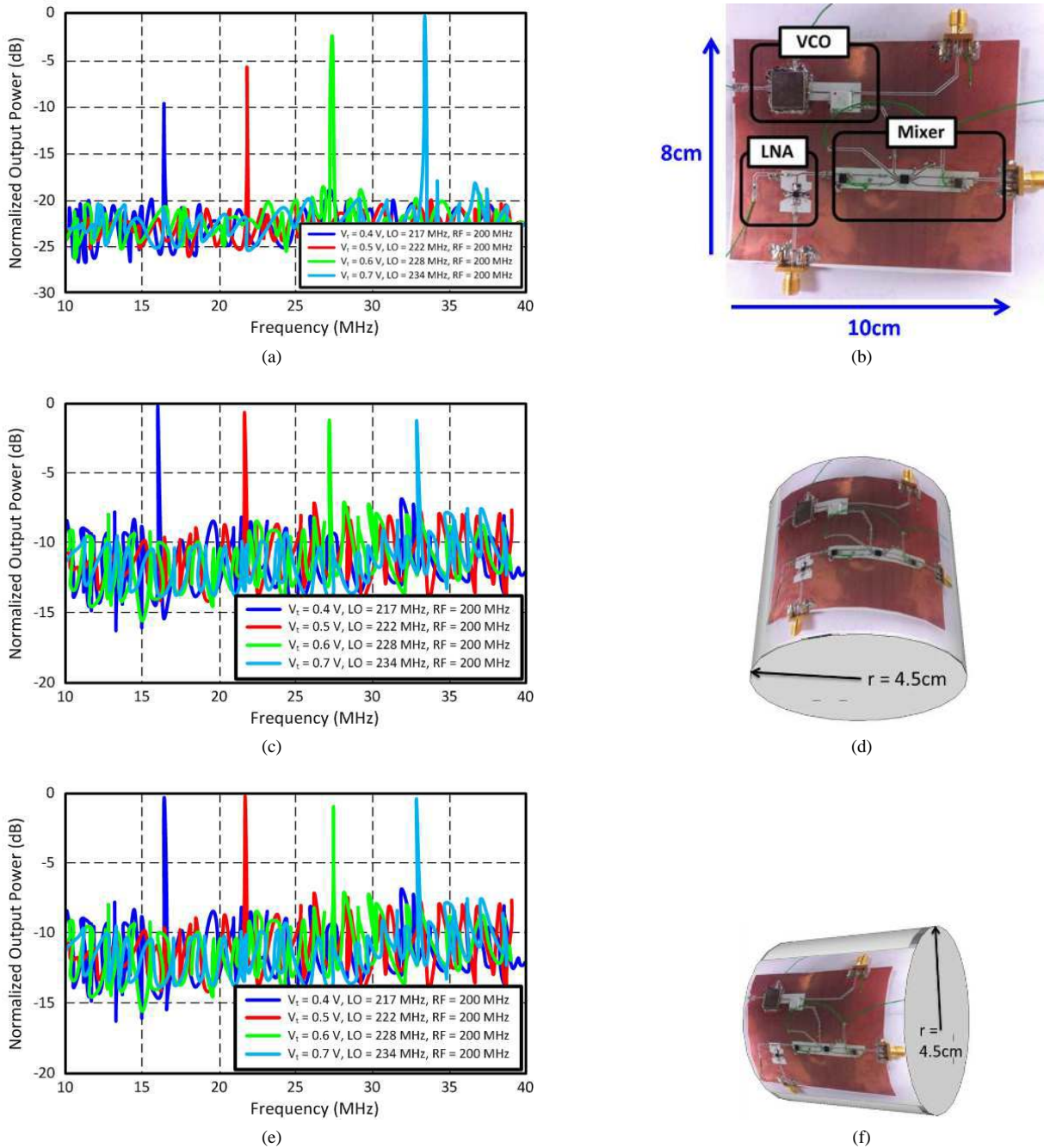


Fig. 29. Output power spectrum and layout/prototype of the flexible GPR module: (a-b) flat, (c-d) curved horizontally and (e-f) curved vertically

(PET) flexible film and measured 10 cm by 8 cm. In the experimental verification stage, the Local Oscillator (LO) frequencies 217 MHz, 222 MHz, 228 MHz and 234 MHz were mixed with an RF input frequency of 200 MHz. The measured beat frequencies (17 MHz, 22 MHz, 28 MHz, 34 MHz) verified the basic functionality of the system (Fig. 29(b)). The system was then rolled around a foam cylinder with a radius of 4.5 cm both horizontally and vertically. The system demonstrated a consistent flex-independent performance without any delamination or cracking (Fig. 29).

*B. Inkjet-Printed Flexible Nodes*

1) *A flexible printed reflection amplifier with enhanced communication capabilities:* Due to its low-power and low-cost nature, backscatter radio is an appealing scheme for use in radio frequency identification (RFID) [50], [51], authentication [52], and sensing applications [53]–[57]. Especially for sensing applications, extended communication ranges are desired; to achieve extended ranges, the backscattered signal’s signal-to-noise ratio (SNR) at the reader has to be boosted. This section presents a preliminary printable flexible prototype for the novel idea of a reflection amplifier that addresses this issue in a very effective way.

When a tag antenna with input impedance  $Z_a$  is connected

to a load  $Z_i$ , the system reflection coefficient is given by Eq. (2).

$$\Gamma_i = \frac{Z_i - Z_a^*}{Z_i + Z_a} \quad (2)$$

$\Gamma_i$  is a complex quantity that determines the amplitude and the phase of the reflected signal from a tag when illuminated by a reader's carrier wave. If for bit "0" a load value of  $Z_0$  is used, and for bit "1" a load value of  $Z_1$  is used, two reflection coefficient values  $\Gamma_0$  and  $\Gamma_1$  will alter the reflected signal accordingly, to achieve binary modulation. The distance  $|\Delta\Gamma| \triangleq |\Gamma_1 - \Gamma_0|$  is of particular importance to the reflected signal's SNR. In [58], where the complete backscatter radio signal model is derived by accounting for both microwave and wireless communication parameters, it can be easily observed that the tag signal SNR at the reader relies on the reflection coefficient distance  $|\Delta\Gamma|$  and the bit duration  $T_b$ :

$$\text{SNR} \propto |\Delta\Gamma|^2 T_b. \quad (3)$$

Thus, a way to increase the tag signal SNR is to increase the bit duration  $T_b$  by reducing the tag bit-rate. For further increase of the SNR though, the quantity  $|\Delta\Gamma|$  has to be maximized.

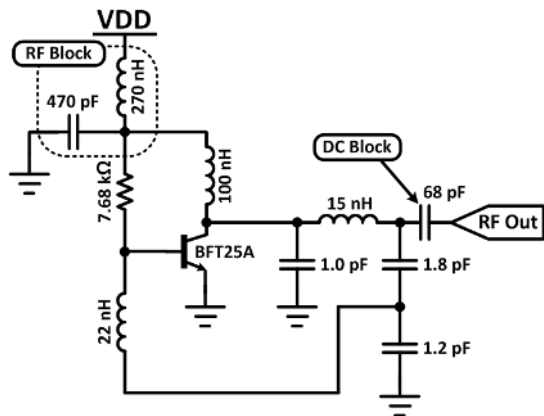


Fig. 30. Reflection amplifier schematic with a common input/output terminal. The amplifier is biased with a low DC voltage to prevent oscillations [59].



Fig. 31. Inkjet-printed flexible reflection amplifier prototype.

Typically, RF tags utilize passive components for binary modulation purposes, which results in reflection coefficient values  $|\Gamma_i| \leq 1$ . This means that increasing the tag SNR by controlling  $\Delta\Gamma$  is bounded by  $|\Delta\Gamma| \leq 2$ . The case  $|\Delta\Gamma| = 2$  corresponds to semi passive tags with antipodal points on the Smith chart (e.g. open and short antenna loads). To override

this bound, non-conventional tag designs have to be utilized, that achieve values of  $|\Gamma_i| > 1$ , i.e. front-ends that feature a reflection gain instead of a reflection loss (as in conventional tags). One novel flexible and rugged implementation of such a system that achieves reflection coefficient amplitudes greater than unity incorporates a reflection amplifier (shown in Fig. 30 and Fig. 31), that increases the amplitude of and reflects incoming signals (Fig. 32). This system also incorporates a phase shifter to alternate the phase of the reflected signal between  $0^\circ$  and  $180^\circ$ , thus achieving binary phase modulation. The total system achieves  $|\Gamma_i| > 1$  for both tag states and  $\Gamma_1, \Gamma_0$  are antipodal; this maximizes  $|\Delta\Gamma|$  for a given reflection amplifier (Fig. 33), significantly increasing the SNR of backscattered signals.

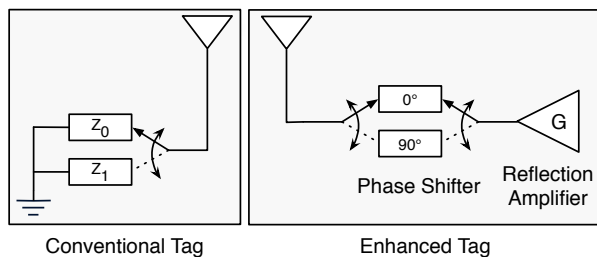


Fig. 32. Left: passive backscattering-based RF tag modulator. Right: Tag with a reflection amplifier and a binary phase shift modulator [59].

The binary phase modulator reflects any incoming signal with two different phase values and attenuated amplitude (due to the switches' insertion loss). The two reflection coefficient values are shown in Fig. 34 for a tag that only employs the phase modulator (both states  $|\Gamma_i| < 1$ ). In the same figure, the two states of the reflection amplifier-phase modulator system are shown: two antipodal reflection coefficient values are achieved, both with amplitude  $|\Gamma_i| \approx 2$ . Specifically, the amplifier-equipped tag achieves  $|\Delta\Gamma| = 4.1$ , in contrast with the modulator-only tag that achieves  $|\Delta\Gamma| = 1.1$ . This corresponds to a tag signal SNR increase of 11.43 dB, which is very beneficial for a significantly increased communication range. For a tag that could otherwise have a very low SNR (order of 0 dB) and would thus be "hidden" from the reader, the 11.43 dB SNR increase could enable the reader to successfully decode it.

An important aspect of the front-ends presented in this section is their low-complexity architecture, which simplifies their implementation. This type of front ends requires only a small number of discrete components and microstrip transmission lines, thus allowing for an easy flexible circuit fabrication using inkjet printing techniques, even on low-cost materials such as photo paper. In Fig. 31, an inkjet-printed flexible reflection amplifier is shown, implemented on paper substrate ( $\epsilon_r = 2.9$ ,  $\tan \delta = 0.045$ , thickness =  $210 \mu\text{m}$ ). In a similar manner, numerous novel backscattering-based RFID-enabled integrated sensing nodes (including control logic, sensors and wireless front-ends) can be fully implemented on flexible substrates by inkjet-printing the required traces and component pads, to minimize the total fabrication cost.

2) *Flexible wireless passive microfluidic sensors*: Flexible printed microfluidic components, such as the ones shown in

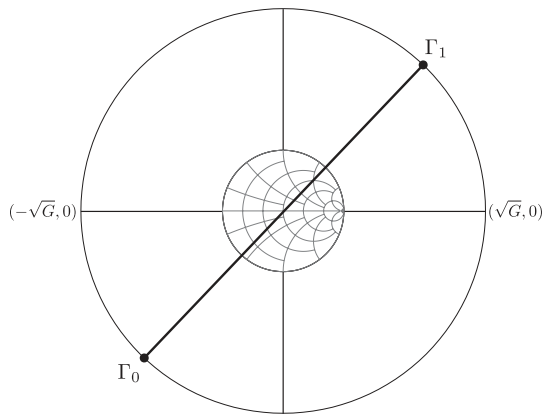


Fig. 33. For a reflection amplifier tag that utilizes a phase shift modulator,  $\Gamma_0$  and  $\Gamma_1$  can both lie far from the unitary circle, maximizing the distance between  $\Gamma_1$  and  $\Gamma_0$  [59].

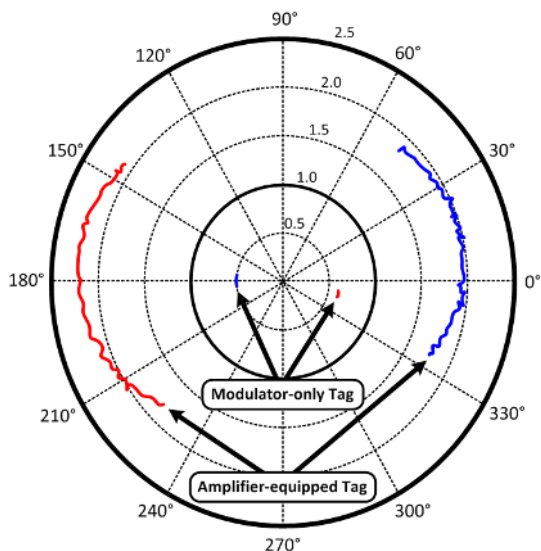


Fig. 34. Comparison of the antipodal reflection coefficient values ( $S_{11}$ ) for a conventional modulator-only tag and an enhanced backscatter efficiency amplifier-equipped tag [59].

Sec. IV-A, can be easily integrated into RFID architectures, similar to the one discussed in Sec. V-B1, to achieve flexible printable zero-power and cable-less sensing platforms. In the benchmarking integrated prototype presented in this section, the RFID-enabled microfluidic tags are designed to operate with a mounted Higgs 3 EPC Gen-2 RFID (Electronic Product Code Generation 2) chip. By effectively varying the capacitive load of a slot placed near the edge of an inkjet printed flexible monopole by utilizing small amounts of different fluids, the electrical length of the antenna will effectively change “on-the-fly”.

Typical passive tags need first to harvest energy fed from the reader before being able to communicate back to it. If the reader does not emit enough power or if too much power is reflected back at the interface between the chip and the antenna, the chip does not receive enough power and cannot turn on. In the “energy harvesting” mode, the tag’s antenna is connected to the energy harvesting circuit and its load

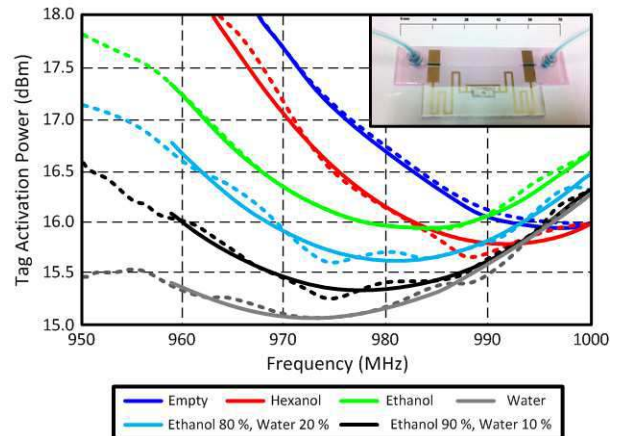


Fig. 35. Wireless measurements of a microfluidic passive tag with a mounted Alien Higgs 3 chip utilizing the Tagformance RFID reader

therefore is  $Z_i = Z_{harvester}^*$  in order to optimize power transfer through the minimization of the reflection coefficient (Eq. (2)). The antenna’s input impedance ( $Z_a$ ) is frequency-dependent while also varying as a function of the antenna length. Only the energy that is not reflected is received by the harvester. Therefore, we can measure the minimum transmitted power required from the reader to turn the tag on over a certain frequency range at a set distance (shown in Fig. 35) in order to indirectly receive information on the value of  $\Gamma$  of the RFID antenna, which is a function of the value of the liquid-dependent  $Z_a$  which is itself related to the length of the antenna and therefore to the permittivity of the liquid.

The flexible sensing platform presented here is universal and can be extended to applications in water quality monitoring, biomedical analysis, and fluid process control.

3) *A flexible WISP-enabled gas sensing node using inkjet printed rGO*: As a proof of concept and without loss of generality, in the presented flexible prototype, the popular WISP (Wireless Identification and Sensing Platform) is connected to the inkjet printed rGO sensing component presented in Sec. IV-B3. The sensor prototype is a battery-free, and programmable RFID tag that can be powered and read by off-the-shelf EPC Gen2 UHF (Ultra High Frequency) RFID readers [44], [60]. It has an on-board micro-controller for sensing and computing functions and is a multi-functional platform. The block diagram of a WISP is shown in Fig. 36, which includes power harvesting, sensor, signal processing, and modulation/demodulation capabilities. The WISP is solely powered by the RF energy transmitted by any commercial RFID reader, which is rectified by a charge pump topology consisting of diodes and capacitors to charge an on-board supercapacitor. Whenever located within the interrogation zone of an RFID reader, the WISP-enabled gas sensor is automatically detected and begins the transmission of the sensed information through the EPC Gen2 protocol.

As the conductivity of the inkjet-printed rGO changes upon exposure to gas, the graphene sensor is used in a resistor divider configuration with a fixed resistor, which is placed across the WISP’s regulated 1.8V and ground traces. When the WISP is interrogated by the reader, the voltage from the

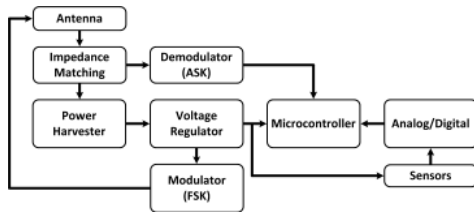


Fig. 36. Block diagram of the WISP RFID-enabled wireless sensor platform.

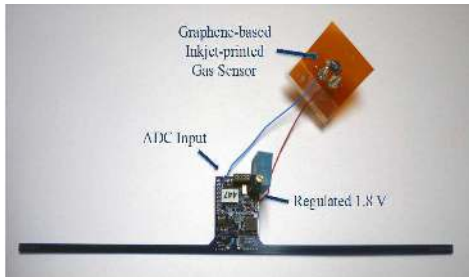


Fig. 37. An rGO-based WISP gas sensor.

voltage divider circuit is read by the WISP’s analog-to-digital converter (ADC), processed, and sent to the reader in the form of an EPC Gen2 packet. Such types of inkjet-printed flexible autonomous wireless sensing modules could set the foundation for the first real-world large-scale Internet of Things and Smart Skin implementations on virtually every flexible substrate.

## VI. MAIN CHALLENGES FOR THE USE OF AMT FOR RF FLEXIBLE COMPONENTS AND MODULES FABRICATION

Starting as a technology once envisioned for completely different applications (namely photoplotting and rapid prototyping), additive manufacturing has seen itself continually evolving to meet ever increasing demands in a direct digital manufacturing (DDM) landscape; yet, despite all the advancements, numerous challenges in materials, deposition methods and IC integration still stand in the way of large-scale flexible inkjet-printed/3D printed high-complexity modules.

### A. Additive Manufacturing Techniques

Additive manufacturing techniques for Radio Frequency Additive Manufacturing (RFAM) can nominally be broken into those that are typically used for metallic traces and those that are used for the dielectrics. This is because the processes and materials used to fabricate conductive traces are typically designed to produce small volumetric deposition rates (on the order of mg/min) for optimized precision and printed feature size ; on the contrary, thick dielectric fabrication with these rates would be too time consuming. Summarized in Table I are a few types of AMTs that lend themselves to RFAM. As can be seen on Table I, inkjet-printing has a low volumetric deposition rate and, as a consequence, is an excellent fabrication method for flexible, thin RF components up to sub-THz frequency bands. However, the combination of inkjet-printing with other RFAM technologies would enable the additive fabrication of a new range of flexible truly 3D low-cost RF integrated modules and systems.

### B. Materials

1) *Dielectrics:* Since the beginning of “rapid prototyping” with stereolithography and other techniques, AM as a whole has mainly focused on the implementation of dielectric structures. Beneficial to the RFAM movement is the fact that previously unrealizable complex geometries and configurations can now be printed with ease. Unfortunately, only a very limited amount of materials and methods have been optimized for high-frequency performance up to now. Many of the standard materials available for use either feature a very high dielectric loss or, as will be detailed in the next section, are unsuitable for some of the standard sintering processes required for SNP (Silver NanoParticles) inks.

AM promise to provide a significantly improved control and accuracy in the fabrication of complex geometries, allowing engineers to envision new ways of achieving desired RF performance and pushing the state-of-the-art by orders of magnitude. One groundbreaking example in this area has been the accurate fabrication of 3D heterogeneous and custom dielectrics for substrates or even lenses [61], [62] by tailoring the effective permittivity of a structure with the inclusion of voxels of air [63]. Furthermore, graded-index (GRIN) lenses, such as Luneburg or Maxwell lenses, can be manufactured with smoother point-to-point index gradients [61].

However, RFAM dielectrics are not without their detractors. As mentioned before, many well understood and developed AM methods use photopolymers as their medium [64]. This works very well for mechanical structures but yields a poor RF performance in regards to the dielectric loss [65]. At this point in time, proper RF dielectrics are a missing link in the fabrication of direct write devices. Advancements in the material extrusion process, mitigation of losses due to photopolymer dielectrics, utilization of some of the other AM techniques (e.g. sheet lamination or binder jetting) and rigorous RF characterization of the deposited materials would result in major leaps forward in the future. Preliminary examples coupling AM with inkjet-printing has led to flexible RF antennas, capacitors and inductors 3D prototypes with acceptable performance up to 10 GHz, demonstrating a potential way to alleviate the high-frequency dielectric-related challenges of AM.

2) *Conductive traces:* Advancements in additively manufactured conductive traces have been substantial in recent years utilizing a variety of conductive materials [66], [67]; however, SNP inks above others have stood out as the preferred solution for conductive trace applications [68], [69]. SNP inks offer good conductivity values, simple post-processing steps and are stable for a relatively long time when stored properly; however, these benefits all come at a cost considering that SNPs can be quite expensive by weight and currently don’t feature any reliable way to be effectively integrated into 3D printed structures.

In commonly utilized inks, SNPs are suspended in a solution that allows the particles not to settle to the bottom just the same as color inkjet inks in the office or home. When printing a pattern, the ink droplet hits the substrate and ideally forms a nicely shaped hemisphere of liquid ink. Once printing is

TABLE I  
ADDITIVE MANUFACTURING TECHNIQUES COMPARED

Additive Technique	Materials	Features size (µm)	Benefits	Drawbacks	Commercial Examples
Material Extrusion	<ul style="list-style-type: none"> <li>Thermoplastics</li> </ul>	100-1000	<ul style="list-style-type: none"> <li>Ultra low-cost</li> <li>Good integration with other AM technologies</li> <li>High volumetric deposition rate</li> </ul>	<ul style="list-style-type: none"> <li>High surface roughness</li> <li>Mediocre feature size</li> <li>Anisotropic parts</li> <li>Unknown material production standards</li> </ul>	<ul style="list-style-type: none"> <li>Stratasys</li> <li>3D Systems</li> <li>Ultimaker</li> </ul>
Stereolithography	<ul style="list-style-type: none"> <li>Photopolymers</li> </ul>	1-100	<ul style="list-style-type: none"> <li>Fine feature size</li> <li>Low surface roughness</li> </ul>	<ul style="list-style-type: none"> <li>RF Lossy materials</li> <li>Difficult to directly integrate with other technology</li> <li>Expensive</li> </ul>	<ul style="list-style-type: none"> <li>Materialise</li> <li>3D Systems</li> </ul>
Material Jetting	<ul style="list-style-type: none"> <li>Photopolymers</li> <li>Waxes</li> <li>Binders</li> </ul>	10-100	<ul style="list-style-type: none"> <li>Fine feature size</li> <li>Good surface roughness</li> <li>Potential integration with inkjet-printed metals</li> </ul>	<ul style="list-style-type: none"> <li>RF Lossy materials</li> <li>Poor integration with other AM technologies</li> <li>Expensive</li> </ul>	<ul style="list-style-type: none"> <li>Objet (Stratasys),</li> <li>3D Systems</li> </ul>
Aerosol Jetting	<ul style="list-style-type: none"> <li>SNP inks</li> <li>Photopolymer resins</li> </ul>	10-100	<ul style="list-style-type: none"> <li>Fine feature size</li> <li>Low surface roughness</li> <li>Multi-material</li> </ul>	<ul style="list-style-type: none"> <li>Only thin layers</li> <li>Low volumetric deposition rate</li> <li>Poor integration with other AM technologies</li> <li>Expensive</li> </ul>	<ul style="list-style-type: none"> <li>Optomec</li> </ul>
Inkjetting	<ul style="list-style-type: none"> <li>SNP inks</li> <li>Photopolymer resins</li> </ul>	10-100	<ul style="list-style-type: none"> <li>Low-cost</li> <li>Fine feature size</li> <li>Multi-material</li> <li>Low surface roughness</li> <li>Medium thickness layers (up to 200 µm)</li> </ul>	<ul style="list-style-type: none"> <li>Medium thickness layers (no more than 200 µm)</li> <li>Low volumetric deposition rate</li> </ul>	<ul style="list-style-type: none"> <li>Dimatix (Fujifilm)</li> </ul>
Syringe Pump	<ul style="list-style-type: none"> <li>SNP inks</li> <li>Any other paste</li> </ul>	100-1000	<ul style="list-style-type: none"> <li>Low-cost</li> <li>Multi-material</li> <li>Good integration with other AM technologies</li> <li>High volumetric deposition rate</li> </ul>	<ul style="list-style-type: none"> <li>Mediocre feature size</li> </ul>	<ul style="list-style-type: none"> <li>nScript/Sciperio</li> </ul>

complete, the ink is sintered using a variety of techniques [70]. The thermal conduction is critical to ink curing as it evaporates the solvent used to carry the SNPs effectively melting the SNP's together, thus enabling a continuous metal trace that can be used for electronics applications [71]. Utilizing the above method, SNPs can obtain good performance results with relatively little additional work featuring conductivity values on the order of bulk metal [72].

However, SNP use features a trade-off. The use of oven sintering techniques naturally works well for substrates that are thermoset or have a high glass transition temperature ( $T_g$ ), such as many of the flexible substrates used for inkjet-printing (Kapton, LCP, paper, etc). Unfortunately, most of the standard materials available for deposition by RFAM either have a  $T_g$  that is often too low for use in an oven (resulting in structure deformation) or very lossy and ill-suited for use as an RF substrate. Furthermore, SNP prices can be in the range of hundreds of dollars per dL, making some applications of this

technique cost-prohibitive.

In comparison to SNP inks, one newly developed ink for the printing of conductive traces is the diamine silver acetate (DSA) ink. DSA offers numerous benefits for flexible electronic applications: low-cost (< \$100/100 mL) compared to SNP inks (> \$100/100 mL), conductivities above 90% bulk silver's and complete sintering at room temperature [73]. Because DSA is relatively new, its true impact and practical limitations have yet to be seen; however, as time progresses DSA may come to supplant SNP as the favored silver deposition method for AMT-manufactured electronic devices.

### C. Component Integration

One method of component integration highlighted by [74] is what is known as self assembly, that can be thought of as the "positioning and bonding of components by random interactions". The method of bonding can vary from electrostatic

to magnetic to chemical; however, the premise remains that it is based on random events that are tailored to result in a desired outcome. Self-assembly is normally thought of in a chemical or nano-level sense; however, in the realm of RFAM it could potentially offer an extremely low-cost method for wireless device fabrication. Self-assembly would not require expensive pick-and-place robotic facilities or infrastructure, but would rather rely on random energy sources (vibration, thermal, etc.) to realize the whole device. For example, [75] demonstrates the effective patterning of a substrate into templates. With the help of vibrations, IC chips dispersed in a fluid are then driven in those templates through a process called “fluidic self-assembly deposition process”. AM, and more specifically RFAM, will require a robust and flexible method of accurately depositing/mounting 2D or 3D structures to be integrated with printed components and substrates. Currently, process planning software is not optimal or even setup to consider the multi-material and embedded component issues that RFAM brings to the table. New technology and software will need to be developed that can handle dielectric, metallic and component level integration all in one suite in order to truly see RFAM lead the way in producing the new generation of easy-to-scale low-cost large-area, flexible RF devices and modules.

## VII. CONCLUSION

This paper has reviewed recent advances and capabilities of inkjet printing on flexible substrates as well as other additive manufacturing techniques for the sustainable ultra-low-cost fabrication of flexible, conformal, wearable and rollable radio frequency (RF)/microwave components, sensors and integrated modules. Numerous examples of flexible inkjet-printed passives, nanotechnology-enabled sensors, microfluidics, energy harvesters, origami reconfigurable components and radar/beacon systems verify the unique capabilities of inkjet printing/additive manufacturing for the implementation of the first real-world truly convergent wireless sensor ad-hoc networks of the future with enhanced cognitive intelligence and “zero-power” operability. Despite the outstanding major challenges for the realization of inkjet-printed/3D printed high-complexity modules, such an approach could feature tremendous potential in numerous future wireless applications requiring very large numbers of flexible RF electronics, such as Internet of Things, Machine-to-Machine (M2M) communication systems, environmentally- friendly (“Green”) RF electronics, “Smart Skins” and “Smart-House” topologies.

## REFERENCES

- [1] E. Cantatore, *Applications of organic and printed electronics*. Springer, 2013.
- [2] A. Nathan, A. Ahnood, M. T. Cole, S. Lee, Y. Suzuki, P. Hiralal, F. Bonaccorso, T. Hasan, L. Garcia-Gancedo, A. Dyadyusha, S. Haque, P. Andrew, S. Hofmann, J. Moultrie, D. Chu, A. Flewitt, A. Ferrari, M. Kelly, J. Robertson, G. Amaratunga, and W. I. Milne, “Flexible electronics: The next ubiquitous platform,” *Proc. IEEE*, vol. 100, no. Special Centennial Issue, pp. 1486–1517, May 2012.
- [3] S. Fuller, E. Wilhelm, and J. Jacobson, “Ink-jet printed nanoparticle microelectromechanical systems,” *J. Microelectromech. Syst.*, vol. 11, no. 1, pp. 54–60, Feb 2002.
- [4] A. Rida, L. Yang, R. Vyas, and M. M. Tentzeris, “Conductive inkjet-printed antennas on flexible low-cost paper-based substrates for RFID and WSN applications,” *IEEE Antennas Propag. Mag.*, vol. 51, no. 3, pp. 13–23, 2009.
- [5] L. Yang, A. Rida, R. Vyas, and M. M. Tentzeris, “RFID tag and RF structures on a paper substrate using inkjet-printing technology,” *IEEE Trans. Microw. Theory Tech.*, vol. 55, no. 12, pp. 2894–2901, 2007.
- [6] B. S. Cook, J. R. Cooper, and M. M. Tentzeris, “Multi-layer RF capacitors on flexible substrates utilizing inkjet printed dielectric polymers,” *IEEE Microw. Wireless Compon. Lett.*, vol. 23, no. 7, pp. 353–355, 2013.
- [7] B. Cook, C. Mariotti, J. Cooper, D. Revier, B. Tehrani, L. Aluigi, L. Roselli, and M. Tentzeris, “Inkjet-printed, vertically-integrated, high-performance inductors and transformers on flexible LCP substrate,” in *2014 IEEE MTT-S Int. Microwave Symp. (IMS)*. IEEE, 2014, pp. 1–4.
- [8] B. Cook, B. Tehrani, J. Cooper, and E. Tentzeris, “Multi-layer inkjet printing of millimeter-wave proximity-fed patch arrays on flexible substrates,” *IEEE Antennas Wireless Propag. Lett.*, 2013.
- [9] B. C. Kjellander, W. T. Smaal, K. Myny, J. Genoe, W. Dehaene, P. Heremans, and G. H. Gelinck, “Optimized circuit design for flexible 8-bit RFID transponders with active layer of ink-jet printed small molecule semiconductors,” *Organic Electronics*, vol. 14, no. 3, pp. 768 – 774, 2013.
- [10] I. Gibson, D. Rosen, and B. Stucker, *Additive Manufacturing Technologies: Rapid Prototyping to Direct Digital Manufacturing*. Springer, 2010.
- [11] Y. Li, R. Torah, S. Beeby, and J. Tudor, “An all-inkjet printed flexible capacitor for wearable applications,” in *2012 Symp. on Design, Test, Integration and Packaging of MEMS/MOEMS (DTIP)*, April 2012.
- [12] J. Lim, J. Kim, Y. J. Yoon, H. Kim, H. G. Yoon, S.-N. Lee, and J. Kim, “All-inkjet-printed Metal-Insulator-Metal (MIM) capacitor,” *Current Applied Physics*, vol. 12, Supplement 1, pp. e14 – e17, 2012.
- [13] G. McKerricher, J. Gonzalez, and A. Shamim, “All inkjet printed (3D) microwave capacitors and inductors with vias,” in *2013 IEEE MTT-S Int. Microwave Symp. Dig. (IMS)*, June 2013, pp. 1–3.
- [14] A. Memicanin, L. Zivanov, M. Damnjanovic, and A. Maric, “Low-cost CPW meander inductors utilizing ink-jet printing on flexible substrate for high-frequency applications,” *IEEE Trans. Electron Devices*, vol. 60, no. 2, pp. 827–832, Feb 2013.
- [15] B. J. Kang, C. K. Lee, and J. H. Oh, “All-inkjet-printed electrical components and circuit fabrication on a plastic substrate,” *Microelectronic Engineering*, vol. 97, pp. 251 – 254, 2012.
- [16] D. Redinger, S. Moles, S. Yin, R. Farschi, and V. Subramanian, “An ink-jet-deposited passive component process for RFID,” *IEEE Trans. Electron Devices*, vol. 51, no. 12, pp. 1978–1983, Dec 2004.
- [17] B. Cook and M. Tentzeris, “A miniaturized wearable high gain and wideband inkjet-printed AMC antenna,” in *Antennas and Propagation Soc. Int. Symp. (APSURSI)*, 2013 IEEE, July 2013, pp. 676–677.
- [18] C. Gabriel, S. Gabriel, and E. Corthout, “The dielectric properties of biological tissues: I. literature survey,” *Physics in medicine and biology*, vol. 41, no. 11, p. 2231, 1996.
- [19] M. Yoo, S. Lim, and M. Tentzeris, “Flexible inkjet-printed metamaterial paper absorber,” in *Antennas and Propagation Society Int. Symp. (APSURSI)*, July 2014, pp. 2060–2061.
- [20] K. J. Vinoy and R. M. Jha, *Radar absorbing materials: From theory to design and characterization*, N. Y. K. Academic, Ed., 1996.
- [21] S. Kim, Y.-J. Ren, H. Lee, A. Rida, S. Nikolaou, and M. Tentzeris, “Monopole antenna with inkjet-printed EBG array on paper substrate for wearable applications,” *IEEE Antennas Wireless Propag. Lett.*, vol. 11, pp. 663–666, 2012.
- [22] N. I. Landy, S. Sajuyigbe, J. J. Mock, D. R. Smith, and W. J. Padilla, “Perfect metamaterial absorber,” *Phys. Rev. Lett.*, vol. 100, p. 207402, May 2008.
- [23] T. Kawase, H. Siringhaus, R. H. Friend, and T. Shimoda, “Inkjet printed via-hole interconnections and resistors for all-polymer transistor circuits,” *Advanced Materials*, vol. 13, no. 21, p. 1601, 2001.
- [24] T. Falat, J. Felba, A. Moscicki, and J. Borecki, “Nano-silver inkjet printed interconnections through the microvias for flexible electronics,” in *2011 11th IEEE Conference on Nanotechnology (IEEE-NANO)*. IEEE, 2011, pp. 473–477.
- [25] I. Reinhold, M. Thielen, W. Voit, W. Zapka, R. Gotzen, and H. Bohlmann, “Inkjet printing of electrical vias,” in *2011 18th European Microelectronics and Packaging Conf. (EMPC)*, Sept 2011, pp. 1–4.
- [26] S. Kim, H. Aubert, and M. Tentzeris, “An inkjet-printed flexible broadband coupler in substrate integrated waveguide (SIW) technology for sensing, RFID and communication applications,” in *2014 IEEE MTT-S Int. Microwave Symp. (IMS)*, June 2014, pp. 1–4.

- [27] H. Friis, C. Feldman, and W. Sharpless, "The determination of the direction of arrival of short radio waves," *Proc. of the Institute of Radio Engineers*, vol. 22, no. 1, pp. 47–78, 1934.
- [28] R. L. Haupt and M. Lanagan, "Reconfigurable antennas," *IEEE Antennas Propag. Mag.*, vol. 55, no. 1, pp. 49–61, 2013.
- [29] S. Yao, S. Georgakopoulos, B. Cook, and M. Tentzeris, "A novel reconfigurable origami accordion antenna," in *2014 IEEE MTT-S Int. Microwave Symp. (IMS)*, June 2014, pp. 1–4.
- [30] A. Thrall and C. Quaglia, "Accordion shelters: A historical review of origami-like deployable shelters developed by the US military," *Engineering Structures*, vol. 59, pp. 686–692, 2014.
- [31] K. Kuribayashi, K. Tsuchiya, Z. You, D. Tomus, M. Umemoto, T. Ito, and M. Sasaki, "Self-deployable origami stent grafts as a biomedical application of Ni-rich TiNi shape memory alloy foil," *Materials Science and Engineering: A*, vol. 419, no. 1, pp. 131–137, 2006.
- [32] W. D. Reynolds, S. K. Jeon, J. A. Banik, and T. W. Murphey, "Advanced folding approaches for deployable spacecraft payloads," in *ASME 2013 Int. Design Eng. Tech. Conferences and Comp. and Inform. in Eng. Conf.* American Society of Mechanical Engineers, 2013.
- [33] X. Liu, S. Yao, S. V. Georgakopoulos, B. S. Cook, and M. M. Tentzeris, "Reconfigurable helical antenna based on an origami structure for wireless communication system," in *2014 IEEE MTT-S Int. Microwave Symp. (IMS)*. IEEE, 2014, pp. 1–4.
- [34] C. Saintsing, B. S. Cook, and M. M. Tentzeris, "An origami inspired reconfigurable spiral antenna," in *ASME Int. Design and Eng. Tech. Conf.*, 2014.
- [35] S. Jalali Mazlouman, A. Mahanfar, C. Menon, and R. G. Vaughan, "A review of mechanically reconfigurable antennas using smart material actuators," in *Proc. of the 5th European Conf. on Antennas and Propagation (EuCAP)*. IEEE, 2011, pp. 1076–1079.
- [36] —, "Reconfigurable axial-mode helix antennas using shape memory alloys," *IEEE Trans. Antennas Propag.*, vol. 59, no. 4, pp. 1070–1077, 2011.
- [37] Q. Ge, C. K. Dunn, H. J. Qi, and M. L. Dunn, "Active origami by 4D printing," *Smart Materials and Structures*, vol. 23, no. 9, p. 094007, 2014.
- [38] W. Su, C. Mariotti, B. S. Cook, S. Lim, L. Roselli, and M. M. Tentzeris, "A metamaterial-inspired temperature stable inkjet-printed microfluidic-tunable bandstop filter," in *2014 European Microwave Conf. (EuMC)*, Rome, Italy, Oct 2014.
- [39] A. Tidar, S. Shafiyoddin, S. Kamble, G. Dharme, S. Patil, P. Khirade, and S. Mehrotra, "Microwave dielectric relaxation study of 1-hexanol with 1-propenol mixture by using time domain reflectometry at 300K," in *2009 Appl. Electromagnetics Conf. (AEMC)*, Dec 2009, pp. 1–4.
- [40] R. Nigmatullin, M. A.-G. Jafar, N. Shinyashiki, S. Sudo, and S. Yagihara, "Recognition of a new permittivity function for glycerol by the use of the eigen-coordinates method," *Journal of Non-Crystalline Solids*, vol. 305, no. 13, pp. 96 – 111, 2002.
- [41] K. Shibata, "Measurement of complex permittivity for liquid materials using the open-ended cut-off waveguide reflection method," in *2011 China-Japan Joint Microwave Conf. Proc. (CJMW)*, April 2011, pp. 1–4.
- [42] V. Lakafosis, X. Yi, T. Le, E. Gebara, Y. Wang, and M. M. Tentzeris, "Wireless sensing with smart skins," in *2011 IEEE Sensors*. IEEE, 2011, pp. 623–626.
- [43] R. Mangu, S. Rajaputra, and V. P. Singh, "MWCNT-polymer composites as highly sensitive and selective room temperature gas sensors," *Nanotechnology*, vol. 22, no. 21, p. 215502, 2011.
- [44] T. Le, V. Lakafosis, Z. Lin, C. Wong, and M. Tentzeris, "Inkjet-printed graphene-based wireless gas sensor modules," in *2012 IEEE 62nd Electron Components and Tech. Conf. (ECTC)*, May 2012, pp. 1003–1008.
- [45] H. Subbaraman, D. Pham, X. Xu, M. Chen, A. Hosseini, X. Lu, and R. Chen, "Inkjet-printed two-dimensional phased-array antenna on a flexible substrate," *IEEE Antennas Wireless Propag. Lett.*, vol. 12, pp. 170–173, 2013.
- [46] A. Georgiadis, A. Collado, S. Kim, H. Lee, and M. Tentzeris, "UHF solar powered active oscillator antenna on low cost flexible substrate for wireless identification applications," in *2012 IEEE MTT-S Int. Microwave Symp. Dig. (IMS)*, June 2012, pp. 1–3.
- [47] S. Kim, A. Georgiadis, A. Collado, and M. Tentzeris, "An inkjet-printed solar-powered wireless beacon on paper for identification and wireless power transmission applications," *IEEE Trans. Microw. Theory Tech.*, vol. 60, no. 12, pp. 4178–4186, Dec 2012.
- [48] A. Traille, A. Coustou, H. Aubert, S. Kim, and M. Tentzeris, "Monolithic paper-based & inkjet-printed technology for conformal stepped-FMCW GPR applications: First results," in *2013 European Microwave Conf. (EuMC)*, Oct 2013, pp. 13–16.
- [49] M. Schlesinger and M. Paunovic, *Modern electroplating*. John Wiley & Sons, 2011, vol. 55.
- [50] *EPC Radio-Frequency Identity Protocols, Class-1 Generation-2 UHF RFID Protocol for Communications at 860MHZ–960MHZ, version 1.2.0*. EPC Global, 2008.
- [51] K. Finkenzeller, *RFID Handbook: Fundamentals and Applications in Contactless Smart Cards, Radio Frequency Identification and Near-Field Communication*, 3rd ed. New York, NY, 10158: John Wiley & Sons, Inc., 2010.
- [52] V. Lakafosis, A. Traille, H. Lee, E. Gebara, M. M. Tentzeris, G. R. DeJean, and D. Kirovski, "RF fingerprinting physical objects for anti-counterfeiting applications," *IEEE Trans. Microw. Theory Tech.*, vol. 59, no. 2, pp. 504–514, 2011.
- [53] G. Vannucci, A. Bletsas, and D. Leigh, "A software-defined radio system for backscatter sensor networks," *IEEE Trans. Wireless Commun.*, vol. 7, no. 6, pp. 2170–2179, Jun. 2008.
- [54] A. Sample, D. Yeager, P. Powlledge, and J. Smith, "Design of a passively-powered, programmable sensing platform for UHF RFID systems," Grapevine, TX, Mar. 2007, pp. 149–156.
- [55] V. Lakafosis, A. Rida, R. Vyas, L. Yang, S. Nikolaou, and M. M. Tentzeris, "Progress towards the first wireless sensor networks consisting of inkjet-printed, paper-based RFID-enabled sensor tags," *Proc. IEEE*, vol. 98, no. 9, pp. 1601–1609, Sep. 2010.
- [56] J. Kimionis, A. Bletsas, and J. N. Sahalos, "Design and implementation of RFID systems with software defined radio," in *6th IEEE European Conf. on Antennas and Propagation (EuCAP)*, Prague, Czech Republic, Mar. 2012, pp. 3464–3468.
- [57] E. Kampianakis, J. Kimionis, K. Tountas, C. Konstantopoulos, E. Koutroulis, and A. Bletsas, "Backscatter sensor network for extended ranges and low cost with frequency modulators: Application on wireless humidity sensing," in *Proc. IEEE Sensors 2013*, Baltimore, MD, Nov. 2013.
- [58] J. Kimionis, A. Bletsas, and J. N. Sahalos, "Increased range bistatic scatter radio," *IEEE Trans. Commun.*, vol. 62, no. 3, pp. 1091–1104, Mar. 2014.
- [59] J. Kimionis, A. Georgiadis, A. Collado, and M. M. Tentzeris, "Enhancement of RF tag backscatter efficiency with low-power reflection amplifiers," *IEEE Trans. Microw. Theory Tech.*, Dec. 2014.
- [60] L. Yang, R. Zhang, D. Staiculescu, C. Wong, and M. Tentzeris, "A novel conformal RFID-enabled module utilizing inkjet-printed antennas and carbon nanotubes for gas-detection applications," *IEEE Antennas Wireless Propag. Lett.*, vol. 8, pp. 653–656, 2009.
- [61] M. Liang, W.-R. Ng, K. Chang, M. E. Gehm, and H. Xin, "An X-band luneburg lens antenna fabricated by rapid prototyping technology," in *2011 IEEE MTT-S Int. Microwave Symp. Dig. (IMS)*. IEEE, 2011, pp. 1–4.
- [62] J. Tribe, W. Whittow, R. Kay, and J. Vardaxoglou, "Additively manufactured heterogeneous substrates for three-dimensional control of local permittivity," *Electronics Letters*, vol. 50, no. 10, pp. 745–746, 2014.
- [63] W. G. Whittow, S. S. Bukhari, L. A. Jones, and I. L. Morrow, "Applications and future prospects for microstrip antennas using heterogeneous and complex 3-D geometry substrates," *Progress In Electromagnetics Research*, vol. 144, pp. 271–280, 2014.
- [64] I. Gibson, D. W. Rosen, and B. Stucker, *Additive manufacturing technologies*. Springer, 2010.
- [65] P. I. Deffenbaugh, R. C. Rumpf, and K. H. Church, "Broadband microwave frequency characterization of 3-D printed materials," in *IEEE Transactions on Components, Packaging and Manufacturing Technology*, vol. 3, no. 12. IEEE, Dec 2013, pp. 2147–2155.
- [66] A. Soltani, T. Kumpulainen, and M. Mantysalo, "Inkjet printed nanoparticle cu process for fabrication of re-distribution layers on silicon wafer," in *2014 IEEE 64th Electronic Components and Technology Conf. (ECTC)*, May 2014, pp. 1685–1689.
- [67] R. Roberts and N. Tien, "Multilayer passive RF microfabrication using jet-printed au nanoparticle ink and aerosol-deposited dielectric," in *2013 Transducers Eurosensors XXVII: The 17th International Conf. on Solid-State Sensors, Actuators and Microsystems (TRANSDUCERS EUROSENSORS XXVII)*, June 2013, pp. 178–181.
- [68] H.-H. Lee, K.-S. Chou, and K.-C. Huang, "Inkjet printing of nanosized silver colloids," *Nanotechnology*, vol. 16, no. 10, p. 2436, 2005.
- [69] B. Cook and A. Shamim, "Inkjet printing of novel wideband and high gain antennas on low-cost paper substrate," *IEEE Trans. Antennas Propag.*, vol. 60, no. 9, pp. 4148–4156, Sept 2012.

- [70] M. L. Allen, M. Aronniemi, T. Mattila, A. Alastalo, K. Ojanperä, M. Suhonen, and H. Seppä, "Electrical sintering of nanoparticle structures," *Nanotechnology*, vol. 19, no. 17, p. 175201, 2008.
- [71] J. R. Greer and R. A. Street, "Thermal cure effects on electrical performance of nanoparticle silver inks," *Acta Materialia*, vol. 55, no. 18, pp. 6345–6349, 2007.
- [72] G. Wiederrecht, *Handbook of nanofabrication*. Academic Press, 2010.
- [73] S. B. Walker and J. A. Lewis, "Reactive silver inks for patterning high-conductivity features at mild temperatures," *Journal of the American Chemical Society*, vol. 134, no. 3, pp. 1419–1421, 2012.
- [74] N. Crane, J. Tuckerman, and G. Nielson, "Self-assembly in additive manufacturing: opportunities and obstacles," *Rapid Prototyping Journal*, vol. 17, no. 3, pp. 211–217, 2011.
- [75] K. Schatz, "Apparatuses and methods facilitating functional block deposition," US Patent 20 070 031 992, August 5, 2007.